OPTIMIZED SYNTHESIS AND CHARACTERIZATION OF *SPIROGYRA* DERIVED ACTIVATED CARBON FOR HIGH PERFORMANCE SUPERCAPACITORS

By

Sami Ullah
Reg. No.: 00000317828
Session 2019-21

Supervised by

Dr. Rabia Liaquat

A thesis submitted to

U.S.-Pakistan Center for Advanced Studies in Energy (USPCAS-E)

in partial fulfillment of the requirement for the degree of

MASTER OF SCIENCE
IN
ENERGY SYSTEMS ENGINEERING

U.S.-Pakistan Center for Advanced Studies in Energy (USPCAS-E)
National University of Sciences and Technology (NUST)
H-12, Islamabad 44000, Pakistan

February 2023

THESIS ACCEPTANCE CERTIFICATE

Certified that final copy of MS/MPhil thesis written by

Mr. **Sami Ullah** **(**Reg. No. 00000317828), of ***U.S.-Pakistan Center for Advanced Studies in Energy (USPCAS-E)*** has been vetted by undersigned, found complete in all respects as per NUST Statues/Regulations, is within similarity indices limit and accepted as partial fulfillment for award of MS/MPhil degree. It is further certified that necessary amendments as pointed out by GEC members of the scholar have also been incorporated in the said thesis.

Signature: _____

Name of Supervisor: Dr. Rabia Liaquat

Date: _____

Signature (HoD): _____

Date: _____

Signature (Dean/Principal): _____

Date: _____

CERTIFICATE

This is to certify that the work in this thesis has been carried out by Mr. **Sami Ullah** completed under my supervision in Biofuels Lab, U.S.-Pakistan Center for Advanced Studies in Energy (USPCAS-E), National University of Sciences and Technology, H-12, Islamabad, Pakistan.

Supervisor: _____

Dr. Rabia Liaquat
USPCAS-E
NUST, Islamabad

GEC member # 1 _____

Dr. Asif Hussain Khoja
Assistant Professor
USPCAS-E
NUST, Islamabad

GEC member # 2: _____

Dr. Mustafa Anwar
Assistant Professor
USPCAS-E
NUST, Islamabad

GEC member # 3: _____

Abeera Ayaz Ansari
Assistant Professor
USPCAS-E
NUST, Islamabad

HoD-ESE: _____

Dr. Rabia Liaquat
USPCAS-E
NUST, Islamabad

Dean/Principal: _____

Dr. Adeel Waqas
USPCAS-E
NUST, Islamabad

ACKNOWLEDGEMENT

First and foremost, praises and thanks to the Almighty ALLAH, for His showers of blessings throughout my research work to complete the research successfully.

I would like to express my deep and sincere gratitude to my supervisor, ***Dr. Rabia Liaquat Associate Professor and Head of Energy Systems Engineering Department, USPCAS-E NUST***, for giving me the opportunity to do research and providing in valuable guidance throughout my research. Her dynamism, vision, sincerity, and motivation have deeply inspired me. She has guided me the methodology to carry out the research and to present the research works as clearly as possible. It was a great privilege and honor to work and study under her guidance. I am extremely grateful for what she has offered me.

I would also like to thank all GEC members, HOD research, management of E.S.E department, all lab engineers, lab technicians of USPCAS-E, NUST for their support throughout this degree program.

I am extremely grateful to my parents, brothers and sisters for their love, prayers, caring and sacrifices for educating and supporting me for my future. I am very much thankful to my wife and my son for their love, understanding, prayers and continuing support to complete this research work.

Finally, I graciously acknowledge the support of this research work by the ***Higher Education Commission (HEC) of Pakistan*** in the grant of "provision of Higher Education opportunities for students of Balochistan & FATA Phase-II".

DEDICATION

First and foremost, I must dedicate this research thesis with limitless thanks to Allah, the Ever-Magnificent; the Ever-Thankful, for His help and bless. I am sure that this work would have never become truth, without His guidance.

I am also dedicating this thesis to my teachers, whom guidance helped me to achieve this status in my life, my loving and caring parents, my inspirations in life who taught me how to face and fight for distinct goals of life, my dearest wife, who leads me through the valley of darkness with light of hope and support, my brothers and sisters and my friends who were always there for me.

ABSTRACT

This study describes the synthesis of *Spirogyra*-derived activated carbon via two key steps of carbonization and activation at optimized temperature using KOH as an activation agent, as well as its application in supercapacitors. *Spirogyra* algae were dried crushed and then carbonized at 450 °C under inert gas environment in a pyrolysis unit followed by activation through KOH at 750 °C in a tube furnace under inert gas environment. Surface structure and morphology of activated carbon were examined using SEM, TGA, XRD, FTIR, Raman spectroscopy, and BET surface area. Specific surface area of Spy-AC-750 calculated was 727.765 m^2g^{-1} with a total pore volume of 0.317 cm^3g^{-1}. CV, GCD, and EIS were conducted to study the electrochemical behavior of the Spy-AC-750 after the coating of synthesized activated carbon on Nickel foam to prepare an electrode. The prepared electrode attained a specific capacitance of 210 Fg^{-1} at a scan rate of $0.5g^{-1}$.These results are the key factors for considering Spy-AC-750 as a good electrode material for energy storage devices. However the low carbon content is the key discouraging aspect of *Spirogyra* algae to use it as a precursor for the synthesis of activated carbon.

Keywords:

Spirogyra Algae, Algal biomass derived activated carbon, Supercapacitor, EDLC, KOH as activating agent, Cyclic Voltammetry, BET analysis,

TABLE OF CONTENTS

CONTENTS

LIST OF FIGURES

LIST OF TABLES

LIST OF ABBRIVATIONS

AC	Activated Carbon
BET	Brunauer, Emmett and Teller
CP	Conducting Polymer
CV	Cyclic Voltammetry
EDLC	Electrolyte Double Layer Capacitor
EDS	Energy-Dispersive X-Ray Spectrometry
EIS	Electrochemical Impedance Spectroscopy
ESD	Energy Storage Device
FTIR	Fourier-Transform Infrared spectroscopy
GCD	Galvanostatic Charge Discharge
LIB	Lithium-Ion Battery
PVDF	Poly-vinylidene-Fluoride
SC	Supercapacitor
SEM	Scanning Electron Microscope
Spy-AC	*Spirogyra* derived Activated Carbon
SSA	Specific Surface Area
TGA	Thermo-Gravimetric Analysis
TMO	Transition Metal Oxides
XRD	X-Ray Diffraction

Chapter 1

Introduction

1.1. Background

One of the most important and basic needs of mankind is energy. In today's modern age, the use of nonrenewable energy resources and other various types of hazardous chemicals is rising day by day to meet the world's sustainable energy demands. The use of limited, non-renewable energy resources and harmful as well as unfriendly environmental chemicals like cadmium (Cd), nickel (Ni), lithium (Li) has motivated the human to invent, renewable and environmentally friendly devices for the energy production and storage. Henceforth, in the modern age to make a sustainable and reliable energy future, non-fossil and renewable based resources of energy have been used.

To harvest and to store energy from these resources, various energy storage technologies are being used. Supercapacitor or electrochemical capacitor and electrolyte double layer capacitors (EDLCs) as energy storage are being considered as a better option from the last two decades [1]. EDCLs are used in a variety of devices that electrostatically store charge on the porous surface of the electrode with a high specific area [2]. More efficient supercapacitors will have a higher power density (HPD), better cyclicity, a faster and reversible charging and discharging rate, and will be safer to use than other traditional batteries [3]. Primarily, the performance and efficiency of a supercapacitor is determined by the materials used in electrode fabrication. Hence, the preparation of cost-effective and environmentally friendly electrode materials can play a vital role in the development of the next generation of EDCLs and supercapacitors [4]. For supercapacitors, conducting polymer [5], carbon [6] and metal oxides [7] are the three most studied materials Because conducting polymers and metal oxides have the property of high specific capacitance, these are used in pseudo-capacitors [3]. However, metal oxides have high costs and low conductive nature [8], while conducting polymers exhibit gradual loss of capacitance as a result of repetitive shrinkage and swelling of the material in the course of charging and discharging[9].

In comparison to other carbon compounds, activated carbon is one of the most common materials used in supercapacitor applications. It has also been used on a commercial scale for the fabrication of electrodes for supercapacitors. Comparatively, some merits of

activated carbon are its low cost, excellent chemical stability, high porosity, large active surface area, easy processibility, and commercial availability [9][10].

At commercial level, the commonly used precursors to produce activated carbon are wood [12], coal [13] and petroleum residues [14]. However, all of these precursors are non-renewable and expensive as well [15]. It can also be produced from various solid carbonaceous natural or synthetic precursors, including biomass[16] and polymers[17]. Natural AC precursors include coconut shells[18], different types of coals[19], peat[20], sugarcane bagasse [21], petroleum coke[22], charcoal[23], algae[24] etc. Algae, as a natural renewable biomass produces abundantly and ubiquitously in the coastal zones of oceans [25] as well as in rivers [26], streams and lakes [27]. Some precursors for the preparation of activated carbon are listed in the Table: 1-1 below.

Table1- 1: Biomass precursors for activated carbon preparation [28]

S.NO	Precursor	Activation Method	Agent
1	Eucalyptus bark	Chemical Activation	H_3PO_4
2	Artocarpusheterophyllus peel	Chemical Activation	H_3PO_4
3	Euryale ferox shell	Chemical Activation	H_3PO_4
4	Mangosteen shell	Chemical Activation	K_2CO_3
5	Paper mill sludge	Chemical Activation	K_2CO_3
6	Hide waste	Chemical Activation	KOH
7	Date pits	Chemical Activation	KOH
8	Corn cob	Chemical Activation	KOH
9	Date stones	Chemical Activation	KOH
10	Dry Okra Wastes	Chemical Activation	KOH
11	safflower bio char	Chemical Activation	$ZnCl_2$
12	tea seed shell	Chemical Activation	$ZnCl_2$
13	cocoa shell	Chemical Activation	$ZnCl_2$
14	rice husk	Chemical Activation	$ZnCl_2$
15	walnut shell	Chemical Activation	$ZnCl_2$
16	chestnut shell	Chemical Activation	$ZnCl_2$
17	sunflower seeds husk	Chemical Activation	$ZnCl_2$
18	apricot stones	Chemical Activation	$ZnCl_2$
19	Azadirachtaindica leaves	Chemical Activation	$ZnCl_2$
20	Ceratoniasiliqua L. residues	Chemical Activation	$ZnCl_2$

In addition to the substrate, biomass-derived AC can be prepared through numerous methods, including physical, chemical, physiochemical, microwave assisted and hydrothermal activation. During the chemical activation method, char that has been pre-impregnated with an activating agent (KOH, K_2CO_3, H_2SO_4, $ZnCl_2$ etc.) is carbonized directly. In this type of activation process, carbon material with high porosity, yield, and specific surface area may be generated within a short time[15].The carbon content of the carbonaceous substance is prepared during carbonization by removing volatile particles via thermal degradation[29]. In carbonization step, the temperature, heating rate, nitrogen gas flow rate, and residence period are all significant factors. Because the obtained biochar has a limited adsorption capacity, an activating procedure is required to increase the pore volume, pore width, and surface area[30]. During the activation process, the disordered carbon was removed first, which exposed the lignin to the activating chemicals and resulted in the formation of the microporous structure. Finally, by burning the walls between the pores, the existing pores are enlarged to a great size. This lowers the amount of micropores by increasing intermediate pores and macro-porosity. Activation can be a technique prior to carbonization or after carbonization for the removal of accumulated tarry substances in biochar, which can aid to improve porosity and give high surface areas for the ACs, depending on the kind of activation[31]. Fig. 1.1depicts various methods of primary activation processes to prepare biomass derived activated carbon.

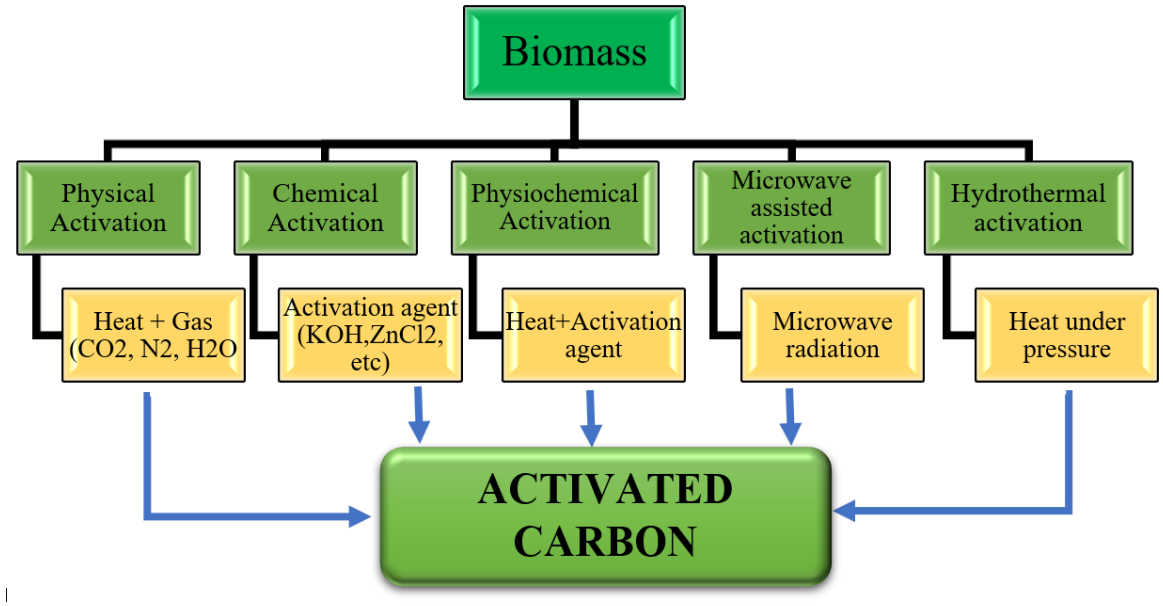

Fig. 1-1: Various methods of the preparation of activated carbon.

The process of activating carbon begins with the removal of tarry particles to remove accumulated tars that restrict pores and helps in enabling the activating agent for later

reaction with biochar[32]. The carbon particles in biochar are then burned before being oxidized with an activating agent. Activation temperature and time are the two most critical characteristics to consider while developing porous structures. These parameters are said to correspond to pore volume, yet they are inversely associated with AC yield.

In literature there are various types (species) of algae like *Pterocladiacapillacea* (red algae), *Undariapinnatifida* (brown algae), *Chlorella vulgaris,Systoceirsstricta, Euphorbia rigida, Enteromorphaprolifera, Spirulinaplatensis, Ulvalactuca* and *turbinariaturbinta* etc. have been used as a precursor for the synthesis of activated carbon using numerous techniques and *parameters* [28][29].Algae is mainly composed of organic contents like cellulose, hemicellulose, starch, alginate, lignin, and inorganic contents which have good plausibility to be used for the preparation of AC. *Spirogyra* Algae are free floatingly filamentous green algae found in freshwater habitats for instance streams, lakes, ponds, rivers, etc.

This research work describe the synthesis of a high-performance activated carbon electrode material using freshwater green algae "*Spirogyra*" derived from a local freshwater stream. *Spirogyra* is photosynthetic green algae which can capture and prepare carbon through the natural process. Therefore, keeping in view, the abundance and easy availability of the *Spirogyra* green algae, practically economic, environmentally safer, and without any practical investments, are the key factors for using this specie of green algae for the preparation of AC in this study. This work also explains the preparation as well as testing parameters and conditions of the activated carbon to enhance the utilization of algal biomass for achieving fruitful results. In addition, biochar was produced by the process of slow pyrolysis in a pyrolysis unit at a temperature of 450°C for 300 minutes, followed by chemical activation using KOH as an activating agent, in a tube furnace at an activation temperature of 750°C. Synthesis and activation procedure of *Spirogyra* derived activated carbon is shown in Fig. 1.2.

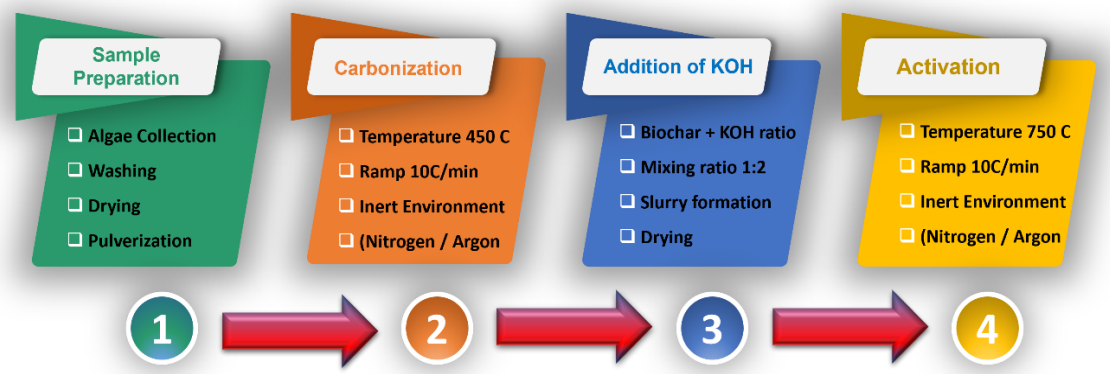

Fig. 1-2: Synthesis of activated carbon procedure

1.2. Problem Statement

Activated carbons are carbonaceous compounds that differ from elemental carbon due to the oxidation of carbon atoms present on the exterior and inner surfaces of carbon materials. The characteristics of activated carbons are large surface areas, well-developed porosity, and tunable surface-containing functional groups. Other than that, they have good kinetic properties and high storage capacities. For these reasons, activated carbons are widely used as electrode materials for supercapacitor to store maximum electrical energy [33]. Activated carbon is also employed as a capturing medium for a variety of toxic gases in order to reduce pollution[34] and has also been shown to be a potential material for water purification [35]. As a result, several compounds have been tested as substitutes for traditional raw materials in the production of activated carbons. Coal, the most often used activated carbon, is a finite, non-renewable resource which is depleting day by day. There is an alternative way to overcome this problem by using renewable sources such as biomass and synthetic wastes precursors. One of these precursors is algal biomass which is cost effective, easily available, and easily process-able. Algae, as a natural renewable biomass produces abundantly and ubiquitously in the coastal zones of oceans [25] as well as in rivers [26], streams and lakes [27].

1.3. Research Objectives

Most of the published research on activated carbon obtained from biomass employs chemical activation. Even though there has been demonstrated remarkable performance of supercapacitor employing AC produced from spore using physical activation and chemical activation. There has been no research on the use of *Spirogyra* algal biomass as a precursor for the synthesis of activated carbon as an electrode material for supercapacitors. Therefore,

the main objective and focus of this thesis are to convert *Spirogyra* biomass into high surface area activated carbon using KOH activation agent by chemical activation and evaluate the algal biomass as electrode material for electrochemical double-layer capacitor (EDLC) applications.

Core objectives of this research are listed below.

- To convert the selected biomass (*Spirogyra* Algae) to high surface area activated carbon (AC) via chemical activation applying KOH as an activation agent.
- To characterize and investigate the prepared ACs' potential as electrode materials for EDLC applications.
- To determine and compare as well as analyze the electrochemical behavior of ACs-derived biomass as electrode materials for EDLC in a strong basic electrolyte (1M, 3M and 6M KOH).

1.4. Scope of the study

To investigate the possibility of producing activated carbon from *Spirogyra* algae. Then, the properties of the activated carbon will be investigated through various techniques. The electrochemical properties of the synthesized activated carbon will be compared to activated carbon already reported in the literature to show the quality of activated carbon and find out if it possible to commercialize it.

1.5. Thesis Structure

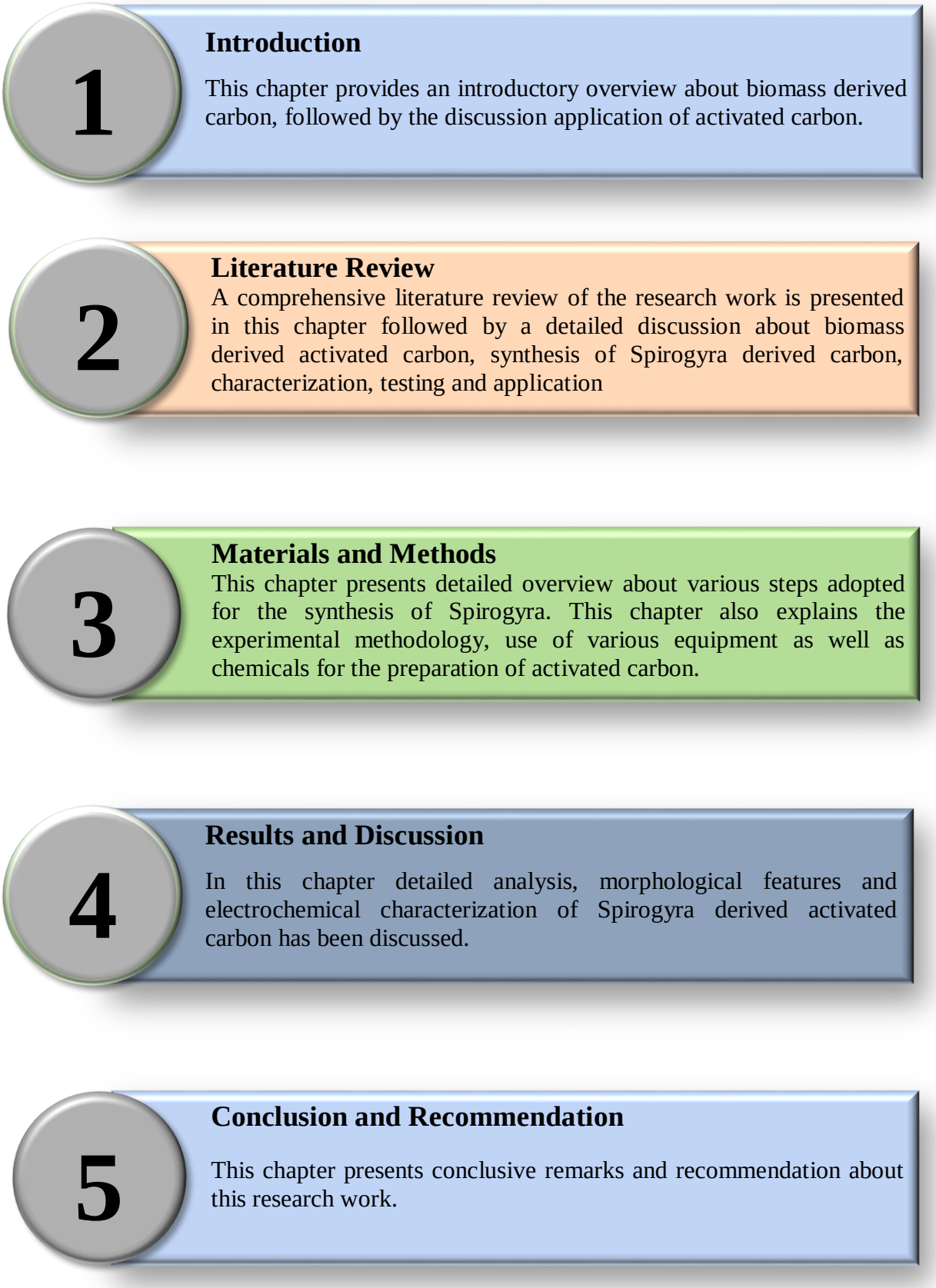

Summary

Supercapacitor or electrochemical capacitor and electrolyte double layer capacitors as energy storage are being considered as a better option from the last two decades. Supercapacitors will have a higher power density (HPD), better cyclicity, a faster and reversible charging and discharging rate, and will be safer to use than other traditional batteries.

Activated carbon (AC) is one of the most common materials used in supercapacitor applications. It can be produced from various solid carbonaceous natural or synthetic precursors, including biomass and algae. AC can be prepared through numerous methods, including physical, chemical, and hydrothermal activation.

High-performance activated carbon electrode material using freshwater green algae "*Spirogyra*" derived from a local freshwater stream. Biochar was produced by the process of slow pyrolysis and chemical activation using KOH as an activating agent, in a tube furnace at an activation temperature of 750°C. Activated carbons are carbonaceous compounds that differ from elemental carbon due to the oxidation of carbon atoms. Activated carbon is widely used as electrode materials for supercapacitor to store maximum electrical energy. The most often used activated carbon material is coal, which is a finite, non-renewable resource which is depleting day by day. There is an alternative way to overcome this problem by using renewable sources such as biomass and synthetic wastes precursors. *Spirogyra* algal biomass could be used as a precursor for the synthesis of activated carbon, which will be used as an electrode material for supercapacitors.

The main objective of this thesis is to investigate the possibility of producing high surface area activated carbon (AC) using KOH as an activation agent. The properties of the activated carbon will be investigated through various techniques.

References

[1] S. Rawal, B. Joshi, and Y. Kumar, "Synthesis and characterization of activated carbon from the biomass of Saccharum bengalense for electrochemical supercapacitors," *J. Energy Storage*, vol. 20, no. October, pp. 418–426, 2018, doi: 10.1016/j.est.2018.10.009.

[2] P. Kossyrev, "Carbon black supercapacitors employing thin electrodes," *J. Power Sources*, vol. 201, pp. 347–352, 2012, doi: https://doi.org/10.1016/j.jpowsour.2011.10.106.

[3] B. Zhu *et al.*, "Tailoring biomass-derived carbon for high-performance supercapacitors from controllably cultivated algae microspheres," *J. Mater. Chem. A*, vol. 6, no. 4, pp. 1523–1530, 2018, doi: 10.1039/c7ta09608a.

[4] G. Wang, L. Zhang, and J. Zhang, "A review of electrode materials for electrochemical supercapacitors," *Chem. Soc. Rev.*, vol. 41, no. 2, pp. 797–828, 2012, doi: 10.1039/c1cs15060j.

[5] G. A. Snook, P. Kao, and A. S. Best, "Conducting-polymer-based supercapacitor devices and electrodes," *J. Power Sources*, vol. 196, no. 1, pp. 1–12, 2011, doi: 10.1016/j.jpowsour.2010.06.084.

[6] F. Béguin, V. Presser, A. Balducci, and E. Frackowiak, "Carbons and electrolytes for advanced supercapacitors," *Adv. Mater.*, vol. 26, no. 14, pp. 2219–2251, 2014, doi: 10.1002/adma.201304137.

[7] W. Wei, X. Cui, W. Chen, and D. G. Ivey, "Manganese oxide-based materials as electrochemical supercapacitor electrodes," *Chem. Soc. Rev.*, vol. 40, no. 3, pp. 1697–1721, 2011, doi: 10.1039/c0cs00127a.

[8] M. Zhi, C. Xiang, J. Li, M. Li, and N. Wu, "Nanostructured carbon-metal oxide composite electrodes for supercapacitors: A review," *Nanoscale*, vol. 5, no. 1, pp. 72–88, 2013, doi: 10.1039/c2nr32040a.

[9] L. Nyholm, G. Nyström, A. Mihranyan, and M. Strømme, "Toward flexible polymer and paper-based energy storage devices," *Adv. Mater.*, vol. 23, no. 33, pp. 3751–3769, 2011, doi: 10.1002/adma.201004134.

[10] F. Cheng, X. Yang, S. Zhang, and W. Lu, "Boosting the supercapacitor performances of activated carbon with carbon nanomaterials," *J. Power Sources*, vol. 450, no. December 2019, p. 227678, 2020, doi: 10.1016/j.jpowsour.2019.227678.

[11] M. Maher, S. Hassan, K. Shoueir, B. Yousif, and M. E. A. Abo-Elsoud, "Activated carbon electrode with promising specific capacitance based on potassium bromide redox additive electrolyte for supercapacitor application," *J. Mater. Res. Technol.*, vol. 11, pp. 1232–1244, Mar. 2021, doi: 10.1016/j.jmrt.2021.01.080.

[12] M. Danish and T. Ahmad, "A review on utilization of wood biomass as a sustainable precursor for activated carbon production and application," *Renew. Sustain. Energy Rev.*, vol. 87, pp. 1–21, 2018, doi: https://doi.org/10.1016/j.rser.2018.02.003.

[13] S. M. Anisuzzaman, C. G. Joseph, Y. H. Taufiq-Yap, D. Krishnaiah, and V. V Tay, "Modification of commercial activated carbon for the removal of 2,4-dichlorophenol

from simulated wastewater," *J. King Saud Univ. - Sci.*, vol. 27, no. 4, pp. 318–330, 2015, doi: https://doi.org/10.1016/j.jksus.2015.01.002.

[14] T. Mochizuki, M. Kubota, H. Matsuda, and L. F. D'Elia Camacho, "Adsorption behaviors of ammonia and hydrogen sulfide on activated carbon prepared from petroleum coke by KOH chemical activation," *Fuel Process. Technol.*, vol. 144, pp. 164–169, 2016, doi: https://doi.org/10.1016/j.fuproc.2015.12.012.

[15] J. Hayashi, T. Horikawa, I. Takeda, K. Muroyama, and F. Nasir Ani, "Preparing activated carbon from various nutshells by chemical activation with K2CO3," *Carbon N. Y.*, vol. 40, no. 13, pp. 2381–2386, 2002, doi: https://doi.org/10.1016/S0008-6223(02)00118-5.

[16] T. Suprianto, Winarto, W. Wijayanti, and I. N. G. Wardana, "Synergistic effect of curcumin and activated carbon catalyst enhancing hydrogen production from biomass pyrolysis," *Int. J. Hydrogen Energy*, vol. 46, no. 10, pp. 7147–7164, 2021, doi: 10.1016/j.ijhydene.2020.11.211.

[17] S. Yenisoy-Karakaş, A. Aygün, M. Güneş, and E. Tahtasakal, "Physical and chemical characteristics of polymer-based spherical activated carbon and its ability to adsorb organics," *Carbon N. Y.*, vol. 42, no. 3, pp. 477–484, 2004, doi: https://doi.org/10.1016/j.carbon.2003.11.019.

[18] G. Wu, B. Jiang, L. Zhou, A. Wang, and S. Wei, "Coconut-shell-derived activated carbon for NIR photo-activated synergistic photothermal-chemodynamic cancer therapy," *J. Mater. Chem. B*, vol. 9, no. 10, pp. 2447–2456, 2021, doi: 10.1039/D0TB02782K.

[19] M. Shi *et al.*, "Coal-derived porous activated carbon with ultrahigh specific surface area and excellent electrochemical performance for supercapacitors," *J. Alloys Compd.*, vol. 859, p. 157856, 2021, doi: https://doi.org/10.1016/j.jallcom.2020.157856.

[20] T. Khadiran, M. Z. Hussein, Z. Zainal, and R. Rusli, "Activated carbon derived from peat soil as a framework for the preparation of shape-stabilized phase change material," *Energy*, vol. 82, pp. 468–478, 2015, doi: https://doi.org/10.1016/j.energy.2015.01.057.

[21] A. O. Abo El Naga, M. El Saied, S. A. Shaban, and F. Y. El Kady, "Fast removal of diclofenac sodium from aqueous solution using sugar cane bagasse-derived activated carbon," *J. Mol. Liq.*, vol. 285, pp. 9–19, 2019, doi: https://doi.org/10.1016/j.molliq.2019.04.062.

[22] D. Zhang, J. Yin, J. Zhao, H. Zhu, and C. Wang, "Adsorption and removal of tetracycline from water by petroleum coke-derived highly porous activated carbon," *J. Environ. Chem. Eng.*, vol. 3, no. 3, pp. 1504–1512, 2015, doi: https://doi.org/10.1016/j.jece.2015.05.014.

[23] Y. Zhang and S.-J. Park, "Incorporation of RuO2 into charcoal-derived carbon with controllable microporosity by CO2 activation for high-performance supercapacitor," *Carbon N. Y.*, vol. 122, pp. 287–297, 2017, doi: https://doi.org/10.1016/j.carbon.2017.06.085.

[24] E.-B. Son, K.-M. Poo, J.-S. Chang, and K.-J. Chae, "Heavy metal removal from

aqueous solutions using engineered magnetic biochars derived from waste marine macro-algal biomass," *Sci. Total Environ.*, vol. 615, pp. 161–168, 2018, doi: https://doi.org/10.1016/j.scitotenv.2017.09.171.

[25] A. El Nemr, O. Abdelwahab, A. Khaled, A. El Sikaily, and A. El Nemr, "Chemistry and Ecology Biosorption of Direct Yellow 12 from aqueous solution using green alga Ulva lactuca Biosorption of Direct Yellow 12 from aqueous solution using green alga Ulva lactuca," *Chem. Ecol.*, vol. 22, no. 4, pp. 253–266, 2006, doi: 10.1080/02757540600812875.

[26] V. Fung and J. D. Ackerman, "The Effects of River Algae and Pore Water Flow on the Feeding of Juvenile Mussels," *J. Geophys. Res. Biogeosciences*, vol. 125, no. 1, p. e2019JG005302, Jan. 2020, doi: https://doi.org/10.1029/2019JG005302.

[27] A. Çelekli, E. Kapı, Ç. Soysal, H. Arslanargun, and H. Bozkurt, "Evaluating biochemical response of filamentous algae integrated with different water bodies," *Ecotoxicol. Environ. Saf.*, vol. 142, pp. 171–180, 2017, doi: https://doi.org/10.1016/j.ecoenv.2017.04.008.

[28] M. S. Reza *et al.*, "Preparation of activated carbon from biomass and its' applications in water and gas purification, a review," *Arab J. Basic Appl. Sci.*, vol. 27, no. 1, pp. 208–238, 2020, doi: 10.1080/25765299.2020.1766799.

[29] N. Radenahmad *et al.*, "A review on biomass derived syngas for SOFC based combined heat and power application," *Renew. Sustain. Energy Rev.*, vol. 119, p. 109560, 2020, doi: https://doi.org/10.1016/j.rser.2019.109560.

[30] X. Yang *et al.*, "Surface functional groups of carbon-based adsorbents and their roles in the removal of heavy metals from aqueous solutions: A critical review," *Chem. Eng. J.*, vol. 366, pp. 608–621, 2019, doi: https://doi.org/10.1016/j.cej.2019.02.119.

[31] K. S. Ukanwa, K. Patchigolla, R. Sakrabani, E. Anthony, and S. Mandavgane, "A Review of Chemicals to Produce Activated Carbon from Agricultural Waste Biomass," *Sustainability* , vol. 11, no. 22. 2019, doi: 10.3390/su11226204.

[32] M. A. Yahya *et al.*, "A brief review on activated carbon derived from agriculture by-product," *AIP Conf. Proc.*, vol. 1972, no. 1, p. 30023, Jun. 2018, doi: 10.1063/1.5041244.

[33] Q. Shi *et al.*, "Preparation of activated carbon from cattail and its application for dyes removal," *J. Environ. Sci.*, vol. 22, no. 1, pp. 91–97, Jan. 2010, doi: 10.1016/S1001-0742(09)60079-6.

[34] N. Abuelnoor, A. AlHajaj, M. Khaleel, L. F. Vega, and M. R. M. Abu-Zahra, "Activated carbons from biomass-based sources for CO2 capture applications," *Chemosphere*, vol. 282, p. 131111, 2021, doi: https://doi.org/10.1016/j.chemosphere.2021.131111.

[35] T. E. Oladimeji, B. O. Odunoye, F. B. Elehinafe, O. Obanla R., and O. Odunlami A., "Production of activated carbon from sawdust and its efficiency in the treatment of sewage water," *Heliyon*, vol. 7, no. 1, p. e05960, 2021, doi: https://doi.org/10.1016/j.heliyon.2021.e05960.

Chapter: 2

Literature Review

Activated carbons are carbonaceous compounds that differ from elemental carbon due to the oxidation of carbon atoms present on the exterior and inner surfaces of carbon materials. The characteristics of activated carbons are large surface areas, well-developed porosity, and high capacity for electrochemical energy storage. It is one of the most commonly used electrode material for many storage devices. The synthesis of activated carbon from *Spirogyra* algal biomass, as well as the characteristics and various testing of the AC, were studied in this study.

2.1. Precursors used for the synthesis of Activated Carbon

In addition to being an electrode material used for many different purposes, activated carbon can be produced from a wealth of different raw materials, making it an incredibly versatile product that can be produced in many different areas depending on what raw material is available. Some of these materials include biomass like shells of plants, banana peels, onion peels, algae, etc., the stones of fruits, woody materials, asphalt, metal carbides, carbon blacks, scrap waste deposits from sewage, and polymer scraps. Different types of coal, which already exist in a carbonaceous form with a developed pore structure, can be further processed to create activated carbon[1].

Although activated carbon can be produced from almost any raw material, it is most cost effective and environmentally conscious to produce activated carbon from waste materials. Activated carbons produced from coconut shells have been shown to have high volumes of micropores, making them the most commonly used raw material for applications where high desorption capacity is needed. Sawdust and other woody scrap materials also contain strongly developed microporous structures which are good for adsorption from the gas phase. Producing activated carbon from olive, plum, apricot, and peach stones yields highly homogenous adsorbents with significant hardness, resistance to abrasion and high micropore volume. PVC scrap can be activated if HCl is removed beforehand, and results in an activated carbon which is a good adsorbent for methylene blue. Activated carbons have even been produced from tire scrap. In order to distinguish between the wide ranges of possible precursors, it becomes necessary to evaluate the resulting physical properties after

activation. When choosing a precursor the following properties are of importance: specific surface area of the pores, pore volume and pore volume distribution, composition and size of granules, and chemical structure/character of the carbon surface. Choosing the correct precursor for the right application is very important because variation of precursor materials allows for controlling the carbons pore structure. Different precursors contain varying amounts of macropores (> 50 nm,) which determine their reactivity. These macropores are not effective for adsorption, but their presence allows more channels for creation of micropores during activation. Additionally, the macropores provide more paths for adsorbent molecules to reach the micropores during adsorption [2]. Precursors which contain a greater amount of volatile substances yield a proportional increase in the reactivity of the activated substance. If the reactivity is too high, the degree of activation can be lowered. Achieving the correct of amount of reactivity is of the utmost importance, since the extent of reaction occurring determines the carbons internal structure [2].

2.2. Various methods used for activated carbon preparation

Various processes and steps have been discussed in literature for the preparation and activation of activated carbon. Some of these are discussed as under. Activated carbon could be prepared through the direct activation of dry raw precursor or through a two-stage process including initial carbonization and then activation. In the two-stage process, the dried raw organic materials such as walnut hulls, wood, bone and coal should be initially carbonized at high temperatures. In the carbonization process, the material should be exposed to a red spot (less than 700 °C) temperature in the distillation apparatus in order to evaporate and remove the hydrocarbons from it in the absence of oxygen. Overall, the process of carbonization is thus a pyrolytic process, and its product is known as carbonized material, char or biochar[1]. After activating the activated carbon, various activation methods are used to further develop porosity and create structures that lead to the formation of fine solid cavities in activated carbon [3]. The pores created on the surface of activated carbon could be categorized as macropores > 25 nm, 1 nm<mesopores < 25 nm, micropores < 1 nm. In view of the nature of the activation process, activated carbon could be prepared in two ways: physical and chemical.

2.2.1. Activated carbon preparation through physical activation

Physical activation used commercially is a two-step process that involves the process of carbonization (pyrolysis) in a neutral atmosphere and then activation in atmospheric

oxidizing gases such as steam, carbon dioxide, carbon dioxide and nitrogen or air mixtures with increasing temperature in the range of 800–1100 °C. This method has the ability to produce activated carbon of porous structure and good physical power, which is an inexpensive method for activated carbon preparation and is considered a green approach because it is chemical-free [4]. However, in the process of the physical activation of activated carbon, the long activation time and low adsorption capacity of prepared activated carbon and its high energy consumption are the main disadvantages.

2.2.2. Activated carbon preparation through chemical activation

Chemical activation, known as wet oxidation, is usually used for raw materials containing cellulose, such as wood, sawdust or fruit pits. These materials are also called biomass resources. In chemical activation for the preparation of activated carbon, organic precursors are activated in the presence of chemicals at high temperatures [1]. For chemical activation, the raw material, in the first stage, is saturated with oxidizing and highly dehydrated chemicals. After impregnation, the suspension is dried and the remaining mixture is heated for a given time. Depending on the activating material and the properties of the final product, activation can take place at temperatures ranging from 400 to 900 °C, at which cellulose is degraded. Eventually, activated carbon is obtained from the repeated washing of the resulting mixture. Another purpose of the final rinse is the recovery of active substances. Chemical activation agents are dehydrating agents that influence pyrolytic decomposition and, by inhibiting the formation of bitumen, increase the activated carbon content and, with subsequent changes in the thermal degradation of precursors, result in the development of the porous structure of carbon materials. These activating agents with deep penetration into the carbon structure lead to the development of small pores in the activated carbon, thereby increasing its surface area [5]. Unlike thermal physical activation, the carbonization and activation phenomena occur simultaneously in the chemical activation so, in contrast to physical activation where carbonization and activation processes are typically performed in two different furnaces, chemical activation can be performed in a single furnace [6].

In the process of chemical activation, the variables that affect the characteristics of the final activated carbon are the amount of impregnation and the weight ratio of chemical agents to dry precursor [2]. Compared to physical activation, this type of activation is more economical because it requires a lower activation temperature, shorter processing time and

higher carbon efficiency. Also, the activated carbon prepared through chemical activation has a more porous structure than that of physical activation. Activated chemicals react with carbon matrices and liberate gas products to form a porous structure [3]. However, the need for a repeated and long washing step to eliminate the spent activator agent from the final mixture at the end of activation process is one of the disadvantages of this method. In addition, toxic wastewater is produced at the washing step, which causes water pollution and therefore requires secondary treatment [6]. The precise selection of the parameters of the chemical activation process is important to the quality of activated carbon production. In addition, in the production of activated carbon, the efficiency of the process is also considered an important factor. In the chemical activation method, the parameters of the chemical agent effect, impregnation ratio and method, temperature, final temperature of carbonization, carbonization time, activation space (under atmospheric conditions) and activation method have been investigated [4]. Different types of chemicals have different reactions with precursors and thus affect the adsorption behavior. The main chemicals which have been used as potential activators are alkaline groups such as potassium hydroxide (KOH), sodium hydroxide (NaOH), calcium chloride ($CaCl_2$) and potassium carbonate (K_2CO_3), acidic groups such as phosphoric acid (H3PO4) and sulphuric acid (H_2SO_4), intermediate metal salts such as $ZnCl_2$ and other activating agents. Based on the physical nature of the activating agent, the activator and precursor could be mixed through two approaches: the physical mixing of the activator and precursor in dry conditions and impregnation [7].

2.2.3. Preparation of activated carbon using various activation agents

2.2.3.1. Activated carbon preparation through activation with phosphoric acid

Among the activating agents, phosphoric acid with the chemical formula H_3PO_4 is widely used in the activation of various lignocellulosic materials [7]. In the reaction of phosphoric acid with lignocellulose since cellulose is resistant to hydrolysis of acid, at the beginning of the mixing of the compounds the acid first reacts with the cellulose and lignin. Activation with phosphoric acid is used in the preparation of activated carbon from various forms of biomass. During the impregnation stage and due to the high polarity of phosphoric acid, controlling the physical and chemical interactions occurring in the bulk of the solution and with the substratum is essential. In this regard, the solution concentration is a primary factor of the activation process with this acid agent. It was found in the activated carbon derived

from pumpkin skin (activation by phosphoric acid) that the pores and cavities formed on the active surface of activated carbon are created due to the evaporation of phosphoric acid during the carbonization process [7]. The main mechanisms of activation with phosphoric acid are the depolymerisation, dehydration and redistribution of biopolymers in lignocellulosic materials. Also, during the activation process, the reaction of phosphoric acid with the active carbon-based precursor leads to the formation of products in the form of particles or volatile substances, which as a result create pores or increase the number of pores in the sites previously occupied by this material. In addition, phosphoric acid leads to the expansion of microporous and mesoporous pores in activated carbon so the activated carbon produced from lignocellulose wastes through activation with phosphoric acid is very porous [8]. Generally, acid refinement leads to an increase in acid groups, eliminates mineral elements and improves the hydrophilic nature of the surface, so the carbon surface will have more access to the aqueous phase. Phosphoric acid has two important functions. However, the excessive amount of phosphoric acid due to the formation of an insulating layer on the activated carbon does not result in the enhancement of porosity on the activated carbon surface [4]. At higher phosphoric acid doses, more potential sites could be created and occupied by the activating agent, which are beneficial to the subsequent pore-opening and -widening processes. However, an excessive increase in phosphoric acid leads to the formation of an insulating layer on the activated carbon investigated the effects of phosphoric acid concentration on the morphology of the activated carbon derived from the core and shells of nuts. The results showed that by increasing phosphoric acid (80% by weight), the highest porosity surface in activated carbon was observed due to the increase in the velocity of the formation of cavities. The outer surface of activated carbon has different vents, while the pore size depends on the amount of carbonization and impregnation. In this case, the whole surface of activated carbon is full of holes and irregular shapes. In a study of activated carbon production from olive stone through activation by 60, 70 and 80% w/w of phosphoric acid, the surface area of the activated carbon increased by increasing the concentration of the acid [3]. It was found that the activated carbon prepared with 80% phosphoric acid had the highest surface area as 1218 m^2/g and pore volume as 0.63 cm^3/g. The results indicated that the increases in the surface area and porosity of activated carbon fiber with acid activation were higher than crude activated carbon, and Fourier-transform infrared spectroscopy (FTIR) showed the significant presence of peaks from different frequencies before and after activation. The results of Brunauer, Emmett and Teller (BET) analysis indicated an increase in the surface area and porosity of activated carbon after acid

activation [9]. It has been shown that the activated carbon prepared with phosphoric acid has less C=O groups than the raw materials. The reduction of carbonyl groups may be due to the effect of H_3PO_4 hydrolysis, which decomposes these groups and other products such as volatile substances. Phosphorus groups are among the most important substances for the adsorption of heavy metals from acidic solutions. H_3PO_4-activated carbon may therefore be considered a cation exchanger for the removal of heavy metal cations from aqueous solutions in the future. Acidic groups are the most derivative of the reaction between phosphoric acid and activated carbon precursor [9]. Activation with phosphoric acid leads to the composition of the phosphorus element in the carbon structure. Phosphoric acid is the most commonly used chemical activator, can produce high porous activated carbon from raw materials and has fewer environmental and toxicological contaminants than potassium hydroxide and zinc chloride. Moreover, phosphoric acid requires a lower activation temperature [10], is not volatile and can form a large number of alkaline or acid-soluble phosphates with elements such as iron, nickel and boron and others that can be incorporated into carbon precursors. It is also confirmed that H_3PO_4 was an effective activator agent, and they observed via carbon electron micrograph scanning electron microscope images that the pores created on the surface of activated carbon are tunnel-shaped and generally have a honeycomb structure. The honeycomb holes of the activated carbon have been fully developed as the corners of the cavities were clearly visible [7]. Acidic purification of activated carbon leads to an increase in the adsorption of various pollutants on the surface due to changes in the chemical surfaces of activated carbon as observed in various articles [10][11], so purification can lead to the removal of hydroxides and the creation of reactive oxygen species groups on activated carbon. Also, the number of acidic functional groups is strongly associated with activated carbon capacity to absorb metal compounds.

2.2.3.2. Activated carbon preparation through activation with Zinc Chloride

Zinc chloride is widely used to produce activated carbon, especially lignocellulosic and cellulosic precursors. Zinc chloride acts as a dampening agent for samples impregnated with this material during activation. Movement of volatile substances through zinc chloride-saturated pores is not disrupted, and after that, during the activation process, volatile substances are released from the surface of activated carbon. Increasing the mass ratio of zinc chloride causes easier release of volatile substances, so the absorption of

nitrogen increases on the activated carbon. Zinc chloride activation induces an electrolytic action called swelling in the molecular structure of cellulose. Inflation causes a breaking down of the cellulose molecules and leads to an increase in different intra- and inter-coated cavities, which causes a higher surface area in the activated carbon. During the activation process, lignocellulosic materials are converted into carbon, and hydrogen atoms, oxygen, carbon monoxide, carbon dioxide, methane and aldehydes are liberated, and diatomaceous distillates are produced. Zinc chloride prevents the formation of bitumen and other fluids that block the surface of carbon monoxide and prevent the movement of volatile substances, and volatile substances are subsequently released from the surface of activated carbon [13]. In activation with zinc chloride, the yield of activated carbon increases due to polymerization by zinc chloride and the creation of a few large-ring aromatic compounds. Since zinc chloride does not react with carbon, the obtained activated carbon has a higher yield than activated carbon produced with potassium hydroxide. Using of zinc chloride leads to the removal of the hydrogen and oxygen atoms from the activated carbon structure. The effect of temperature and amount of zinc chloride on various atoms is that the content of hydrogen and oxygen decreases while nitrogen increases [14]. Zinc chloride acts as a Lewis acid and enhances the condensed aromatic reactions by facilitating molecular hydrogen deformation from the hydro-aromatic structure of precursors so, through the exclusion of some of the active sites from the adjacent molecules, polymerization reactions occur and are affected. By increasing the amount of zinc chloride, more cracks may occur in the structure of activated carbon, so the productivity may decline, resulting in an increase in the mesoporosity of the activated carbon structure. It can be said that by increasing the weight ratio of zinc chloride, the structure breaks down and the micropores deform and become mesopores [15]. Increasing the amount of zinc chloride leads to the removal of volatile compounds from the activated carbon structure, so the number of acidic groups is reduced. It has also been reported that by increasing zinc chloride, the phenolic and carboxylic groups are also affected, while the lactone groups are not. Then, during activation with zinc chloride, phenolic and carboxylic groups are reduced, while lactone groups are increased [16]. By increasing the amount of zinc chloride activating agent, the percentage of carbon and mesopores in the structure of the prepared activated carbon is increased. Cavities on the surface of the activated carbon result from the evaporation of spaces occupied by zinc chloride during the carbonization process, so chloride is an active agent in producing activated carbon with a high surface area and provide higher adsorption capacity [17]. In a study [18], it was observed that the BET surface area and micropore and

mesopore volumes of activated carbon prepared increased by increasing the amount of zinc chloride in the initial activator/precursor mixture. Moreover, by increasing the amount of zinc chloride, the removal of tar from the activated carbon structure was increased, as was the release of volatiles[14]. Although zinc chloride is an excellent activating agent in activated carbon preparation, it is seldom used in the food and pharmaceutical industries due to its health-related problems [10].

2.2.3.3. Activated carbon preparation through activation with Potassium Carbonate

Potassium carbonate with the chemical formula K_2CO_3 is a well-known activating agent in the production of activated carbon [7]. Potassium and sodium hydroxide have adverse effects, but potassium carbonate is not harmful if used for food supplements (often used as supplementary food supplements) [20]. Potassium carbonate is known to be a better activating agent than potassium hydroxide due to the production of activated carbon with higher yield, higher surface and pore volume, and higher capacity for adsorbing large molecules like methylene blue from aqueous solutions showed that the activated carbon produced by potassium carbonate had higher yields than the activated carbon produced by potassium hydroxide. Also, under the same conditions, the specific surface area of the activated carbon produced from potassium carbonate is more than the carbon produced from potassium hydroxide. In addition, the activated carbon produced from potassium carbonate has lower ash and sulphur content than the activated carbon produced from potassium hydroxide [21].

2.2.3.4. Activated carbon preparation through activation with potassium hydroxide

In recent years, potassium salts such as KOH and K2CO3 have been widely used in the production of low-cost activated carbon[22]. Among the various activators, potassium hydroxide has been extensively used, due to its ability to produce activated carbon with a high surface area, its distribution of fine pore size under the same conditions, low environmental pollution, less corrosiveness and lower cost[23]. The chemical activation of phosphoric acid and zinc chloride is used to activate lignocellulosic materials that have not previously been carbonized, while metal compounds such as potassium hydroxide are used to activate the precursors of coal [24]. It is reported that activated carbon with potassium

hydroxide has the highest efficiency in the adsorption of heavy metals compared to other activators [25]. Cavities formed in activated carbon are the result of the evaporation of potassium hydroxide from places previously occupied by this activator [21]. KOH activator is an activating agent rapidly saturated with precursors and does not evaporate completely, so its activation temperature is generally lower than the boiling point of KOH (1327 °C) [23]. KOH-activated carbon has a higher surface area and pore volume, but typically has lower yield (10–40%) compared to other activators such as $ZnCl_2$ and H_3PO_4 [26]. During activated carbon activation with alkali substances, alkali metals and carbonates are created which, in the carbon matrix, are responsible for the stability and expansion of the spaces between the carbon-atom layers and, as a result, increase the efficiency and adsorption capacity of activated carbon [27]. Activated carbon produced from potassium hydroxide has a higher microporous structure than activated carbon produced from sodium hydroxide [21]. By increasing the dosage of potassium hydroxide, microporous pores develop on the surface of the activated carbon, while the mesoporous pores decrease due to the characteristics of the potassium hydroxide activators [28]. The results of a study showed that chemical activation for the preparation of activated carbon from municipal waste with potassium hydroxide (2 M) significantly [29].

1. Increased the surface area and the total pore volume.
2. Modified the number of functional groups on the surface.
3. Increased the removal of arsenic in a shorter time.
4. Improved the arsenic adsorption capacity.

The possible reactions that may occur during the activation process with potassium hydroxide are presented in equations 1–4 as follows.

$$2KOH \rightarrow K_2O + H_2O \quad (1)$$

$$C + H_2O \rightarrow H_2 + CO \quad (2)$$

$$CO + H_2O \rightarrow H_2 + CO_2 \quad (3)$$

$$K_2O + CO2 \rightarrow K_2CO_3 \quad (4)$$

Activated carbon with potassium hydroxide is oxidized in alkaline medium with high oxygen content [29]. In strong activation with a high amount of potassium hydroxide, carbon atoms are eliminated from the internal structure of carbon, and the BET surface area increases with the formation of a porous structure .Oxygenated functional groups as active

sites are able to interact with other molecules in adsorption applications [23]. By increasing the activation temperature of potassium hydroxide, the surface area of activated carbon and the number of oxygen groups of activated carbon increase [22]. Generally, by increasing the impregnation ratio of potassium hydroxide to char, the surface area of the activated carbon increases, but if the amount of potassium hydroxide is about eight times greater, the walls between pores formed on activated carbon are further degraded so the surface area is reduced [14]. Increasing the concentration of potassium hydroxide activator, the dehydration and degradation of the mesopores and their conversion to larger pores probably lead to a decrease in the adsorption capacity of activated carbon [5]. The reactions of carbon with alkali metal activators are presented in equations 5 and 6 as follows [29].

$$6NaOH + 2C \leftrightarrow 2Na + 3H_2 + 2Na_2CO_3 \quad (5)$$

$$6KOH + 2C \leftrightarrow 2K + 3H_2 + 2K_2CO_3 \quad (6)$$

Potassium metal is thought to be introduced into the internal structure of the carbon matrix during the gasification process, leading to the expansion of existing pores and the creation of new ones [2]. Therefore, increasing the amount of potassium hydroxide plays a key role in porosity modeling. Porosity expands successfully, and micro- and mesopores are formed in the off-centre walls of the pores, which increases the BET surface area and pore volume [10]. Activation with potassium hydroxide can also be accomplished through direct chemical activation (physical mixing) or impregnation with activated chemicals. In direct chemical activation, in the first stage activated carbon precursors get saturated, moisture is removed and activation occurs at the desired ratio (KOH weight is greater than precursor weight). Precursor carbonization is often eliminated when the solid impregnation method is considered [9]. By increasing activation, a large amount of potassium hydroxide is typically used, and the weight ratio of KOH to carbon is in the range of 3–7 in most cases. This not only increases the cost of preparation of materials but also increases the potential for environmental hazards caused by potassium hydroxide, the corrosiveness of the process of washing with acid solutions, which results in using other appropriate methods (such as potassium induction as an activation agent by ion exchange) for activation with potassium hydroxide [17]. Also, in the char impregnation method with KOH, potassium hydroxide molecules are readily in contact with the surface of the char, thus leading to a higher degree of micro and mesoporosity. At the stage of washing the activated carbon, a significant amount of potassium hydroxide is introduced into the aquatic media before use. Some studies have focused on the significant concerns regarding the release of spent potassium

hydroxide residues during activation, in terms of either environmental risks or their recovery potential after activation [12]. The mechanism of the potassium hydroxide reaction is described by Radovic and Rodriguez-Reinoso. In this mechanism, potassium hydroxide is converted to K_2O at the beginning of the dehydration process (step 1), and then K_2O is converted to metallic potassium (step 2) [8]. The free potassium then penetrates the grapheme layers and causes the structural expansion of the grapheme layers. Moreover, various potassium compounds produce after a series of reactions during activation with potassium hydroxide, oxidation and hydration. The carbon produced with chloride acid 0.1 N and water is then washed to remove K, K_2O, K_2CO_3 and KOH residues from the graphene layers. However, potassium carbonate will decompose during the activation process and CO_2 will be emitted. The reaction between the activating agent and the precursor of carbon materials results in the decomposition of volatile organic compounds, thus creating a porous surface on the surface of the activated carbon samples [21]. Among the alkali metals, potassium hydroxide and sodium hydroxide are effective activators in producing activated carbon. Among the alkaline metals, KOH is the most effective factor for producing activated carbon. Researchers have been able to provide convincing descriptions of the activated carbon activation process with KOH [2]. The results showed that sodium hydroxide has a lower efficiency than potassium hydroxide in the chemical activation of activated carbon, which is due to the different performances of metal hydroxides in the activation of activated carbon [13]. Although potassium hydroxide increases the pore surface, potassium hydroxide-saturated activated carbon is less efficient than activated carbon saturated with zinc chloride or phosphoric acid, so activating with potassium hydroxide requires a high temperature (greater than 650 °C) and carbon content is less than constant carbon in the precursor. In this condition, the potassium metal is placed in the carbon matrix, with activated carbon efficiency lower than the carbon content of the raw material [28][29]. The use of KOH as an active agent is to produce activated carbon with a narrow pore size distribution and the development of effective porosity. It is believed that the activation mechanism with alkali metals such as KOH relies on the fact that alkali metals act as an input catalyst in the carbon network, an electron donor, during the reaction to gas (gasification) [30]. Also, using KOH as an activator has been proposed for environmental compatibility with $ZnCl_2$ [26]. Generally, chemical activation with alkaline groups leads to an increase in the positive charge on activated carbon, which is desirable to absorb contaminants with a negative charge [30]

2.2.3.5. Activated carbon preparation through activation with other activating agents

Table 2.1 shows the prepared activated carbon from various agricultural materials and activated with various uncommon activating agents

Table 2-1: Biomass precursors and activation agents for the synthesis of activated carbon

S.No.	Precursor	Activation Agent
1	Kenaf core	$K_2C_2O_4$
2	Ramuls mori	$N_2H_9PO_4$
3	Rice straw	$N_2H_9PO_4$
4	Coffee husk	$FeCl_3$
5	Sunflower oil cake	H_2SO_4
6	Date stones	$FeCl_3$
7	Rice husk	$CuCl_2$
8	Date pits	$FeCl_3$
9	Apricot stones	H_2SO_4
10	Waste tea	$C_2H_3O_2K$

2.3. Energy storage devices

Energy storage devices (ESDs) with high energy and power densities have always been a key factor in making greater use of renewable energy sources and integrating them into the current energy infrastructure for modern society's development. Low-cost, high-capacity ESDs are essential for the development of high-performance hybrid electric cars, fully electric vehicles, laptops, and smartphones. Two measures are used to compare different types of ESDs: energy, or the potential to perform function, and power, or the rate at which energy is generated.

The specific gravimetric/volumetric/areal energy may be determined to characterize the amount of energy stored per unit mass/volume/area and is used to define the energy density. Specific energy and specific power are the energy density and power density per unit mass, respectively, in this thesis. The energy and power densities of a number of commonly used

energy storage devices are depicted in a simple Ragone plot shown in Fig. 2-1. Supercapacitors (SCs) are a hybrid form between traditional capacitors and batteries, having higher specific energy and specific power than standard capacitors and batteries, respectively. Lithium-ion batteries (LIBs) are popular because they transform chemical energy into electricity and have a high energy density, but their power is limited by the kinetics of the chemical process. Long charging-discharging cycles, high power capabilities, and a wide operating temperature range are just a few of the benefits SCs have over LIBs [29]. Supercapacitors, on the other hand, have a lower energy density than LIBs. As a result, it is desirable to improve the energy density of supercapacitors without compromising their high-power density.

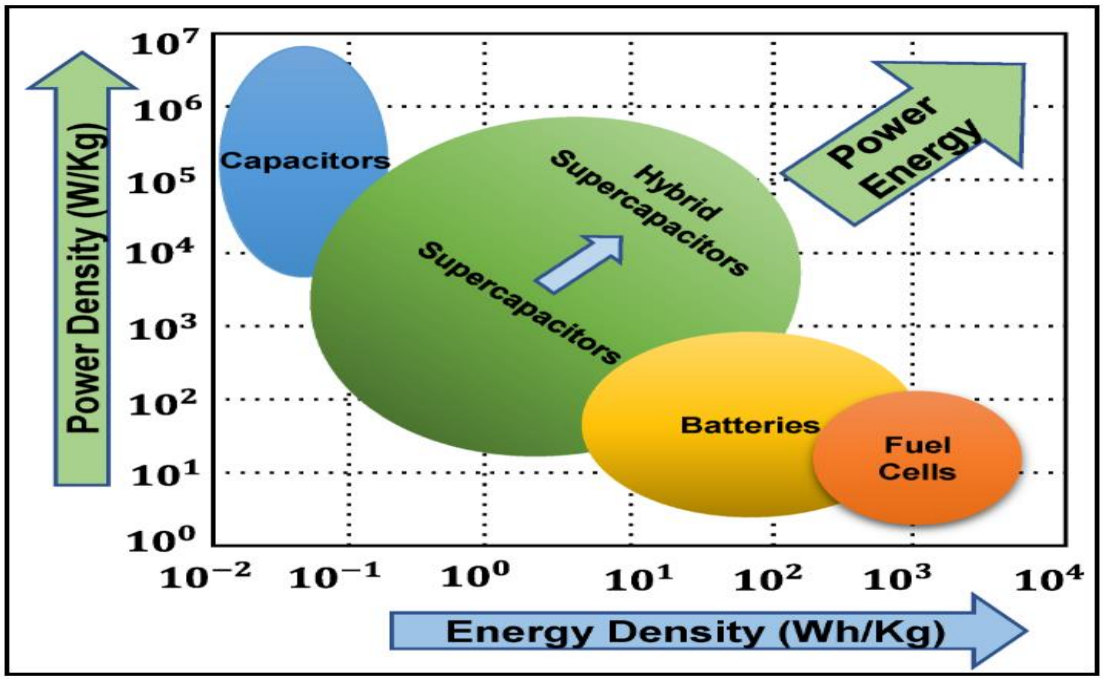

Fig. 2-1: Ragone Plot of various energy storage devices [27]

2.3.1. Supercapacitors and Electric Double layer Capacitors (EDLCs)

Electrochemical double layer capacitors (EDLCs), pseudo-capacitors, and hybrid capacitors (a combination of EDLCs and pseudo-capacitors) are the three types of SCs based on their energy storage processes. Even though the processes of these three are varied, they all have a similar structure. SCs are made up of two electrodes that have been immersed in electrolyte as shown in Fig. 2-1. In contrast to the conventional capacitors, which use dielectric layers to store energy, electric double layers are formed at the interfaces between the electrolyte and the electrodes to store energy; current collectors (usually high conductive materials), are directly connected to the external circuit; and a separator, which

is a thin, porous, non-conductive, and ion-permeable film, is placed between the two electrodes to prevent short circuit.

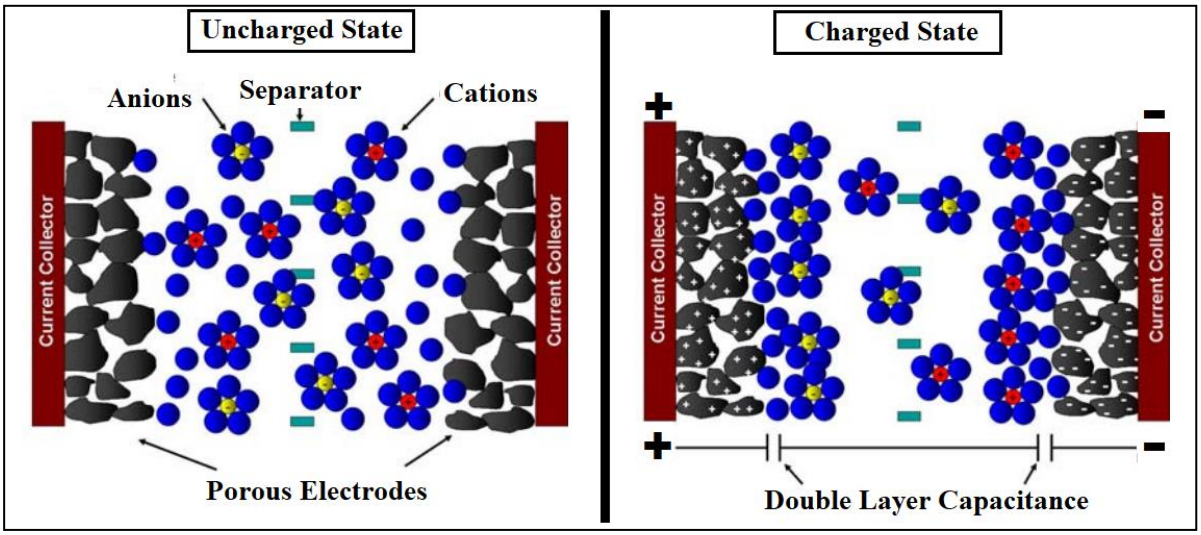

Fig. 2-2: Structure of Supercapacitor [30]

EDLCs have relatively long cycle lives because their energy storage is determined by the accumulation of electric charge at the electrode/electrolyte interface. Their performance is influenced by several factors, including electrical field intensity, electrolyte ions and solvent, and chemical affinity between adsorbed ions and electrode surface. The two electrodes of EDLCs, also known as symmetrical supercapacitors, are always comprised of the same materials. Because of no redox processes, the terms "anode" and "cathode" are not used for EDLCs.

2.3.2. Pseudo-capacitors

Pseudo-capacitors, which are based on quick and reversible Faradaic redox processes on the surface of electro-active species such metal oxides, metal-doped carbons, or conductive polymers [28], have higher energy densities than EDLCs but have a shorter cycle life and a lower charging rate. Its energy storage process is comparable to that of batteries, but its electrochemical processes are faster. Due to the fact that all pseudo-capacitors contain two layers, the electrostatic double-layer capacitance is also included. As there are two different electrode materials are used in pseudo-capacitors and hybrid capacitors, therefore asymmetric structures are commonly employed. As a result, in asymmetric supercapacitors, the operating voltage ranges of the positive and negative electrodes are different, and the total voltage window can be wider than in symmetric supercapacitors, thus increasing the energy density of SCs. One thing that EDLCs and pseudo-capacitors

have in common is that energy storage takes place mostly in the material at the electrolyte-electrode contact. As a result, by providing a high surface area, lowering particle size can possibly boost the use of active materials. It is widely known that high-performance supercapacitors may be made by developing ultrathin nanostructures with a size of less than 10 nm[31]. However, a balance between specific surface area and pore size of electro-active materials is preferred because large microporosity (leading to poor conductivity) and a wide distribution of pore sizes will cause a dramatic loss of capacitance, especially at high current densities[32]. Conducting polymers (CPs) and transition metal oxides (TMO) are always used to produce pseudo-capacitances. CPs are conjugated carbon chains that are semi-conducted. After the doping procedure, CPs might become conductive. Polyaniline, being an inexpensive, highly conductive, and readily produced material with a high doping rate during charging and discharging, has piqued the interest of researchers working on high capacitance supercapacitors [33]. Furthermore, its well-bonded and flexible structure eliminates the need for additional binders or conductive chemicals. Polypyrrole [34], ethylenedioxythiophene, and polythiophene are some more commonly utilized CPs (PTh). The structural breakdown that occurs during redox reactions, on the other hand, invariably results in a short cycle life. TMOs, such as ruthenium oxides (RuO_2) [9], manganese oxides (MnO_2), and iridic oxide (IrO_2), have been proposed for SCs. TMOs have the benefit of being able to switch readily between a series of continuous redox reactions due to the transition metals' various oxidation states. Specific capacitance (Cs) has been reported to be as high as 1100 F/g[10], which is 4-5 times higher than that of AC-based SCs. TMOs, on the other hand, have a low conductivity.

2.3.3. Hybrid capacitors

Depending on the configuration of the electrode materials, hybrid capacitors, which are a combination of EDLCs and pseudo-capacitors, can serve as asymmetric capacitors and composite capacitors at the same time [35]. Combining carbon-based materials with pseudo-capacitive nanomaterial having high power density, i.e., adding polymers and/or high energy density TMOs, is an efficient way to boost the energy density of SCs without losing power density or cycle stability [36]. Due to the desirable hierarchical porous pathways with superior mechanical durability and high conductivity, it has been established that the intertexture can have a synergistic influence on electrochemical performance [37]. Other ways to increase the performance of carbon-based EDLCs include incorporating other elements like nitrogen and sulphur into the carbon-based materials [38]. The surface

property of carbon-based materials may be modified by the oxygen functional group to increase wettability in aqueous electrolytes and improve electrochemical performance [39].In conclusion, putting pseudo-capacitive materials into the carbon network can provide a synergistic effect that improves the electrochemical performance of EDLCs significantly. However, the high expenses of developing such complex systems, as well as the difficulties of purification, prevent hybrid-supercapacitors from being used in practical applications.

Summary

This chapter presents a detail literature review about reported materials, methods and application of activated carbon for supercapacitors. Various types of reported precursors used for the synthesis of activated carbon have been discussed. This discussion further extends the coverage toward the details about the preparation methods of activated carbon as well as various activation agents. In the last part of the chapter different types of capacitors has also been discussed in detail.

References

[01] R. Kötz and M. Carlen, "Principles and applications of electrochemical capacitors," *Electrochim. Acta*, vol. 45, no. 15, pp. 2483–2498, 2000, doi: https://doi.org/10.1016/S0013-4686(00)00354-6.

[02] D. Xu, C. Xuan, X. Li, Z. Luo, et al., Novel helical carbon nanotubes-embedded reduced graphene oxide in three-dimensional architecture for high-performance flexible supercapacitors, Electrochimica Acta. 339 (2020) 135912, https://doi.org/ 10.1016/j.electacta.2020.135912.

[03] R. Liu, S. Sun, R. Zhong, et al., Nitrogen-doped microporous carbon coated on carbon nanotubes for high performance supercapacitors, Micropor. Mesopor. Mat. (2020) 110300, https://doi.org/10.1016/j.micromeso.2020.110300.

[04] M. Cossutta, V. Vretenar, T.A. Centeno, et al., A comparative life cycle assessment of graphene and activated carbon in a supercapacitor application, J. Clean. Prod. 242 (2020) 118468, https://doi.org/10.1016/j.jclepro.2019.118468.

[05] S. Zhang, K. Tian, B.H. Cheng, et al., Preparation of N-doped supercapacitor materials by integrated salt templating and silicon hard templating by pyrolysis of biomass wastes, ACS Sustain. Chem. Eng 5 (8) (2017) 6682–6691, https://doi.org/ 10.1021/acssuschemeng.7b00920.

[06] M. Genovese, J. Jiang, K. Lian, N. Holm, High capacitive performance of exfoliated biochar nanosheets from biomass waste corn cob, J. Mater. Chem. A. 3 (2015) 2903–2913, https://doi.org/10.1039/C4TA06110A.

[07] Y.S. Yun, M.H. Park, S.J. Hong, M.E. Lee, Y.W. Park, H.J. Jin, Hierarchically porous
carbon nanosheets from waste coffee grounds for supercapacitors, ACS Appl. Mater. Inter. 7 (6) (2015) 3684–3690, https://doi.org/10.1021/am5081919.

[08] Q. Zhang, K. Han, S. Li, M. Li, J. Li, K. Ren, Synthesis of garlic skin-derived 3D hierarchical porous carbon for high-performance supercapacitors, Nanoscale 10 (5) (2018) 2427–2437, https://doi.org/10.1039/C7NR07158B.

[09] F. Liu, Z. Wang, H. Zhang, et al., Nitrogen, oxygen and sulfur co-doped hierarchical porous carbons toward high-performance supercapacitors by direct pyrolysis of kraft lignin, Carbon 149 (2019) 105–116, https://doi.org/10.1016/j. carbon.2019.04.023.

[10] K. Yan, L.B. Kong, K.W. Shen, et al., Facile preparation of nitrogen-doped hierarchical porous carbon with high performance in supercapacitors, Appl. Surf. Sci. 364 (2016) 850–861, https://doi.org/10.1016/j.apsusc.2015.12.193.

[11] S. Xu, B. Cao, B.B. Uzoejinwa, E.A. Odey, S. Wang, et al., Synergistic effects of catalytic co-pyrolysis of macroalgae with waste plastics, Process Saf. Enviro. 137 (2020) 34–48, https://doi.org/10.1016/j.psep.2020.02.001.

[12] M. Lakshmikandan, A.G. Murugesan, S. Wang, et al., Sustainable biomass production under CO2 conditions and effective wet microalgae lipid extraction for biodiesel production, J. Cleaner Prod. 247 (2020) 119398, https://doi.org/ 10.1016/j.jclepro.2019.119398.

[13] Y. Wang, Q. Qu, S. Gao, G. Tang, K. Liu, S. He, et al., Biomass derived carbon as binder-free electrode material for supercapacitors, Carbon 155 (2019) 706–726, https://doi.org/10.1016/j.carbon.2019.09.018.

[14] J. Yan, Q. Wang, T. Wei, Z. Fan, Recent Advances in Design and Fabrication of Electrochemical Supercapacitors with High Energy Densities, Adv. Energy Mater 4 (2014), 1300816, https://doi.org/10.1002/aenm.201300816.

[15] Y.C. Liu, B.B. Huang, X.X. Lin, Z.L. Xie, Biomass-derived hierarchical porous carbons: boosting the energy density of supercapacitors via an ionothermal approach, J. Mater. Chem. A 5 (2017) 25090, https://doi.org/10.1039/C7TA90265D.

[16] Z. Bi, Q. Kong, Y. Cao, G. Sun, F. Su, X. Wei, Biomass-derived porous carbon materials with different dimensions for supercapacitor electrodes:a review, J. Mater. Chem. A 7 (2019) 16028, https://doi.org/10.1039/C9TA04436A.

[17] H. Lu, X.S. Zhao, Biomass-derived carbon electrode materials for supercapacitors, Sustain. Energy Fuels 1 (2017) 1265–1281, https://doi.org/10.1039/C7SE00099E.

[18] N. Yadav, Promila Ritu, S.A. Hashmi, Hierarchical porous carbon derived from eucalyptus-bark as a sustainable electrode for high-performance solid-state supercapacitors, Sustain. Energy Fuels 4 (2020) 1730–1746, https://doi.org/10.1039/C9SE00812H.

[19] A. Jain, S.K. Tripathi, Fabrication and characterization of energy storing supercapacitor devices using coconut shell based activated charcoal electrode, Mat. Sci. .Eng.: B 183 (2014) 54–60, https://doi.org/10.1016/j.mseb.2013.12.004.

[20] J. Chmiola, G. Yushin, Y. Gogotsi, C. Portet, P. Simon, P.-L. Taberna, Anomalous increase in carbon capacitance at pore sizes less than 1 nanometer, Science 313 (2006) 1760–1763, https://doi.org/10.1126/science.1132195.

[21] B.E. Conway, Electrochemical Supercapacitors: Scientific Fundamentals and Technological Applications, first ed., Springer, New York, 1999.

[22] F. Beguin, E. Frackowiak, Supercapacitors: Materials, Systems, and Applications, first ed., Wiley-VCH Verlag, Singapore, 2013.

[23] J. Zhang, J. Xue, P. Li, S. Huang, H. Feng, H. Luo, Preparation of metal-organic framework-derived porous carbon and study of its supercapacitive performance, Electrochim. Acta 284 (2018) 328–335, https://doi.org/10.1016/j.electacta.2018.07.102

[24] B. Barati, K. Zeng, J. Baeyens, et al., Recent progress in genetically modified microalgae for enhanced carbon dioxide sequestration, Biomass Bioenerg. 145 (2021) 105927, https://doi.org/10.1016/j.biombioe.2020.105927.

[25] S. Xu, J. Chen, H. Peng, et al., Effect of biomass type and pyrolysis temperature on nitrogen in biochar, and the comparison with hydrochar, Fuel. 291 (2021) 120128, https://doi.org/10.1016/j.fuel.2021.120128.

[26] W. Chen, H. Yang, Y. Chen, et al., Transformation of nitrogen and evolution of Ncontaining species during algae pyrolysis, Environ. Sci. technol. 51 (11) (2017) 6570–6579, https://doi.org/10.1021/acs.est.7b00434.

[27] M. Wayu, “Manganese Oxide Carbon-Based Nanocomposite in Energy Storage

Applications," *Solids* , vol. 2, no. 2. 2021, doi: 10.3390/solids2020015.

[28] M. A. Ben Fathallah, A. Ben Othman, and M. Besbes, "Modeling a photovoltaic energy storage system based on super capacitor, simulation and evaluation of experimental performance," *Appl. Phys. A*, vol. 124, Jan. 2018, doi: 10.1007/s00339-018-1549-x.

[29] M. D. Stoller, S. Park, Y. Zhu, J. An, and R. S. Ruoff, "Graphene-Based Ultracapacitors," *Nano Lett.*, vol. 8, no. 10, pp. 3498–3502, Oct. 2008, doi: 10.1021/nl802558y.

[30] V. Manisha, P. Tonya, and J. Li, "Supercapacitors: Review of Materials and Fabrication Methods," *J. Energy Eng.*, vol. 139, no. 2, pp. 72–79, Jun. 2013, doi: 10.1061/(ASCE)EY.1943-7897.0000102.

[31] H. Jiang, P. S. Lee, and C. Li, "3D carbon based nanostructures for advanced supercapacitors," *Energy Environ. Sci.*, vol. 6, no. 1, pp. 41–53, 2013, doi: 10.1039/C2EE23284G.

[32] H. Zhang, G. Cao, Z. Wang, Y. Yang, Z. Shi, and Z. Gu, "Tube-covering-tube nanostructured polyaniline/carbon nanotube array composite electrode with high capacitance and superior rate performance as well as good cycling stability," *Electrochem. Commun. - Electrochem COMMUN*, vol. 10, pp. 1056–1059, Jul. 2008, doi: 10.1016/j.elecom.2008.05.007.

[33] L. Benhaddad, J. Gamby, L. Makhloufi, A. Pailleret, F. Pillier, and H. Takenouti, "Improvement of capacitive performances of symmetric carbon/carbon supercapacitors by addition of nanostructured polypyrrole powder," *J. Power Sources*, vol. 307, pp. 297–307, Mar. 2016, doi: 10.1016/j.jpowsour.2015.12.007.

[34] H. Jiang, T. Zhao, C. Li, and J. Ma, "Hierarchical self-assembly of ultrathin nickel hydroxide nanoflakes for high-performance supercapacitors," *J. Mater. Chem.*, vol. 21, no. 11, pp. 3818–3823, 2011, doi: 10.1039/C0JM03830J.

[35] C. D. Lokhande, D. P. Dubal, and O.-S. Joo, "Metal oxide thin film based supercapacitors," *Curr. Appl. Phys.*, vol. 11, no. 3, pp. 255–270, 2011, doi: https://doi.org/10.1016/j.cap.2010.12.001.

[36] K. Naoi and P. Simon, "New Materials and New Configurations for Advanced Electrochemical Capacitors," *Electrochem. Soc. Interface*, vol. 17, Mar. 2008, doi: 10.1149/2.F04081IF.

[37] J. Yan *et al.*, "Advanced Asymmetric Supercapacitors Based on Ni(OH)2/Graphene and Porous Graphene Electrodes with High Energy Density," *Adv. Funct. Mater.*, vol. 22, pp. 2632–2641, Jun. 2012, doi: 10.1002/adfm.201102839.

[38] D. Zhu *et al.*, "Nitrogen-containing carbon microspheres for supercapacitor electrodes," *Electrochim. Acta*, vol. 158, pp. 166–174, 2015, doi: https://doi.org/10.1016/j.electacta.2015.01.155.

[39] T. Cai, M. Zhou, D. Ren, G. Han, and S. Guan, "Highly ordered mesoporous phenol–formaldehyde carbon as supercapacitor electrode material," *J. Power Sources*, vol. 231, pp. 197–202, Jun. 2013, doi: 10.1016/j.jpowsour.2012.12.072.

Chapter 3

Material and Methodology

3.1. Precursor selection

Worldwide, algal biomass and agricultural biomass wastes are readily available; the only need is to develop a method for the preparation of low-cost activated carbon. There are various types (species) of algae like Pterocladiacapillacea (red algae)[1], Undariapinnatifida (brown algae)[2], Chlorella vulgaris[3],[4], Systoceirsstricta[5], Euphorbia rigida[6], Enteromorphaprolifera[7], Spirulinaplatensis[8], Ulvalactuca[9] and turbinariaturbinta[10] etc. have been used as a precursor for the synthesis of activated carbon using numerous techniques and parameters. Algae is mainly composed of organic contents like cellulose, hemicellulose, starch, alginate, lignin and inorganic contents which have good plausibility to be used for the preparation of AC[11]. *Spirogyra* Algae are free floatingly filamentous green algae found in fresh water habitats for instance streams, lakes, ponds, rivers, etc. [12]. So, increasing attention has been given to cost-effective techniques like slow pyrolysis of biomass and its conversion into carbonaceous materials like biochar and then activated carbons (ACs) for electrochemical applications. So, the selection of material and its preparation was done by extensive literature.

The main parameters used to select the most appropriate precursor for the synthesis of activated carbon for electrochemical application are surface area, textural characteristics, physical and chemical properties along with durability, availability, reliability, and adaptability aspects [13],[14]. Properties of activated carbon in the sense of electrochemical application are mainly based on the preparation and characterization parameters like surfaces and textural properties (high carbon content, high surface area, high pore volume and porosity, thermal stability, functional groups, and adsorption ability) which help to choose the activated carbons for electrochemical energy storage purpose. There are many techniques and apparatus have been developed to analyze these properties.

A comprehensive level of research has been carried out for the preparation of activated carbons (ACs) from a vast variety of carbon-comprising source materials including almond shell, coconut shell, palm shell, sugarcane bagasse, corn cob, and rice husk, as well as

various types of algal biomass [15][18]. Considering the above prospects, the present work involves the synthesis of surface modified ACs using *Spirogyra* algae as a precursor through the processes of slow pyrolysis at carbonization stage and high temperature stage of activation with KOH. And then prepared AC was used systematically as electrode material for the electrochemical applications in supercapacitors.

3.2. Materials & chemicals

Spirogyra fresh water green filamentous algae were used as a raw material for the preparation of biochar and then activated carbons. For this study the green algae *Spirogyra* was collected from a local freshwater stream in district Bajaur. The obtained algae were given a wash to remove impurities like sand particles and then dried at open space under sun for 48 hours. This dried algae was crushed into powder of size (<2mm) by using the grinder (Sundy, China) as shown in Fig. 3.4 then stored for further processes.

H_2SO_4, KOH, HCl (Sigma-Aldrich manufactured), distilled and de-ionized water (Vitro Diagnostic Laboratories) were the key chemicals and washing media used in this work. The specifications of chemicals and washing media used in the synthesis process of activated carbon are listed in Table 3.1. The instruments and equipment used for the preparation and processing of activated carbon were autoclave/pyrolysis unit, alumina combustion boats, horizontal gas flow tube furnace, magnetic hot-plate & stirrer, grinder and sieves of different sizes.

Table 3.1: Specification of chemical and solvents used for the synthesis of activated carbon

S.No.	Chemicals/Solvent	Specifications
1	Potassium Hydroxide (KOH)	Specification of pH, Eur, BP, NF Assay85% Impurities10-12% Heavy metals (as Pb) 0.003% K_2CO_3 3.5%
2	Sulphuric Acid (H_2SO_4)	Density 1.84
3	De-ionized Water (H_2O)	
4	Distilled Water (H_2O)	pH Maintained at 25 °C Resistivity >2.0 Mega Ohm/cm

3.3. Preparation steps of activated carbon

Synthesis of activated carbon using *Spirogyra* algae as a precursor comprises various steps. These steps include Collection of algae, sun-drying, pulverization, carbonization, addition of activation agent, activation, washing, drying, and storing. Stepwise processes flow diagram of *Spirogyra* derived activated carbon from the algae collection to the prepared activated carbon is shown in the following Fig. 3.1.

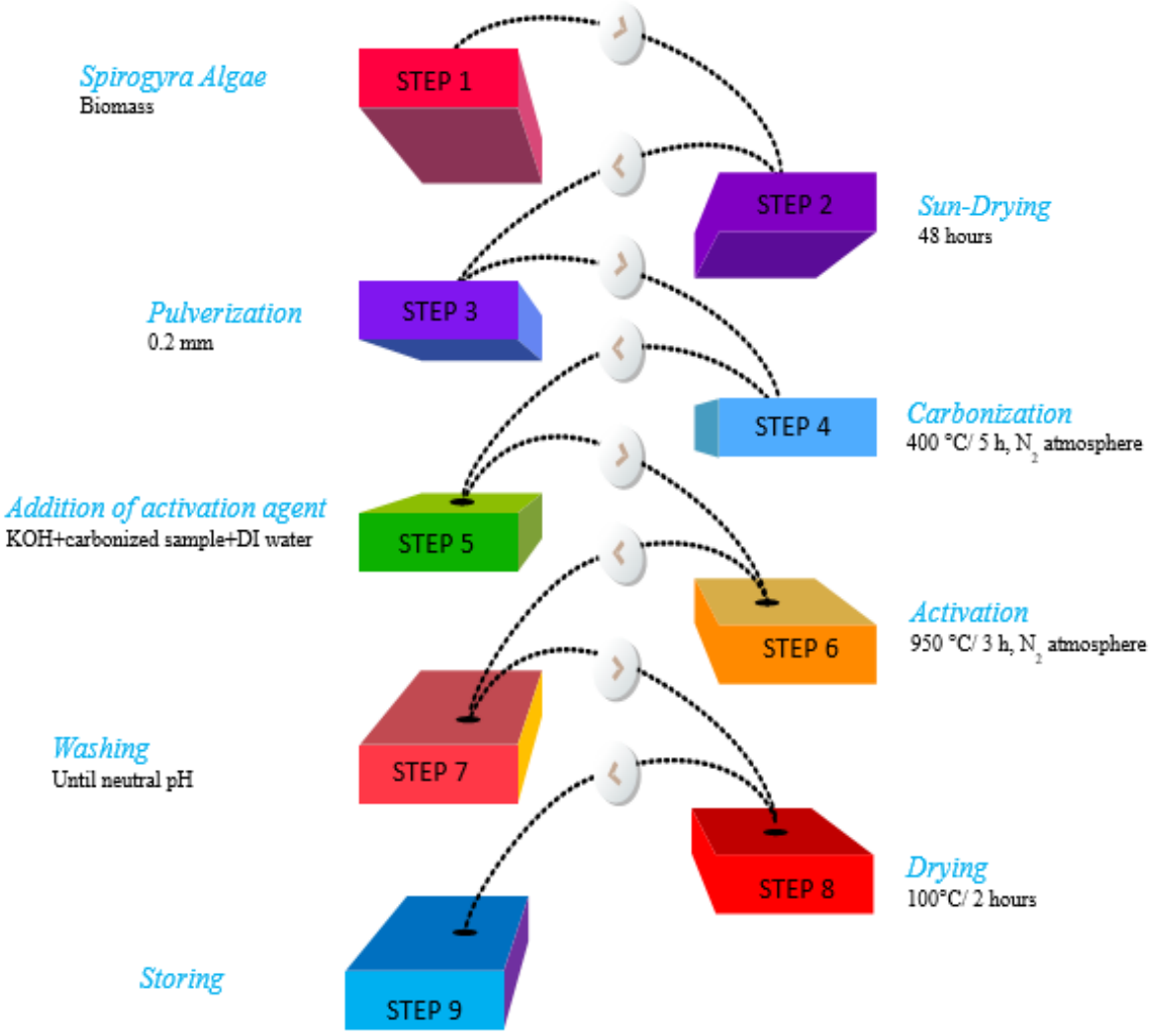

Fig. 3-1: Preparation steps of activated carbon

3.3.1. Collection of algae

The green algae *Spirogyra* was collected from a local freshwater stream in district Bajaur and washed with tap water repeatedly following by washing with distilled water to remove all the impurities, grasses, and sand particles. Fig. 3.2 shows collected freshwater washed green algae.

Fig. 3-2: *Spirogyra* green algae

3.3.2. Sun-Drying of algae

Washed and cleaned algal biomass was kept in the open space for complete drying in the sun. At this stage, all the humidity in the sample had almost dried. Dried *Spirogyra* algae is shown in the Fig. 3-3.

Fig. 3-3: *Spirogyra* green algae in dry form

3.3.3. Pulverization of dried algae

The dried sample was pulverized into powder form up-to a size of 0.02 mm using a grinder and sieved as shown in Fig. 3.4. After pulverization two steps technique was applied for the preparation of activated carbon.

Fig. 3-4: Pulverized Algae

3.3.4. Carbonization of pulverized algae

During this step, a 50-gram pulverized sample of algae was carbonized for 5 hours at 450°C with a 10°C/minute ramping rate in an alumina crucible inside a pyrolysis unit as shown in Fig. 3.5. N_2 gas was supplied to provide an inert atmosphere during the process of carbonization at 110 mL/minute flow rate. After 5 hours of heating at 450°C, the pyrolysis unit was cooled to room temperature, and the carbonized sample was removed. Using a mortar and pestle, the carbonized sample was pulverized to form a fine powder and kept in a dry vial. Steps detail for the preparation of *Spirogyra* derived activated carbon in this work is shown in Fig.3.1. On the same process total 4 samples of algae were carbonized.

Fig. 3-5: Temperature controller of pyrolysis unit

3.3.5. Addition of activating agent

During this step all carbonized samples were mixed one by one by continuous stirring (150rpm) with KOH in 15 ml distilled water at 65°C for 300 minutes to make slurry. Weight ratio for mixing carbonized sample and KOH was 1:2. Then the slurry was dried at 85 °C for 14 hours in drying oven to evaporate water from the sample. Dried sample (Carbonized algal biomass+KOH) was crushed with mortar and pestle for making powder form of the sample.

3.3.6. Activation of carbonized samples

The second step of the experiment was the activation of the carbonized sample. During this step, each carbonized sample was mixed by continuous stirring (450 rpm) with KOH in 15 mL of distilled water at 65°C for 300 minutes to make slurry. The weight ratio for mixing the carbonized sample and KOH was 1:2. The slurry was then completely dried in an oven at 85°C for 6 hours. The dried sample (Carbonized algae+ KOH) ground into a fine powder with a mortar and pestle and then kept in a tube furnace (GSL-1800X-KS60 of MTI Corporation USA) applying high temperatures as 700°C, 750°C, 800°C and 850°C for 120 minutes with 10°C/min ramp rate in an inert environment of N_2 for activation as shown in Fig. 3.6. The tube furnace was allowed for cooling to room temperature after 120 minutes. Then each sample was rinsed with diluted HCL and then by deionized water repeatedly until approaching neutral pH level. Activated carbon prepared during these attempts were marked as Spy-AC-700, Spy-AC-750, Spy-AC-800 and Spy-AC-850 and then stored.

Fig. 3-6: Tube Furnace

3.3.7. Washing of activated carbon

After the complete activation, the sample was rinsed with diluted HCL repeatedly until the pH level approached neutral.

3.3.8. Drying of activated carbon

Then after washing, all samples were kept in an oven (Shel Lab High Performance Forced Air Laboratory Oven (SMO10HP-2))at 60 ℃ for 2 hours for complete drying.

Fig. 3-7: Prepared Activated Carbon

3.3.9. Storing of activated carbon

Completely dried samples were stored in a bottle for further testing and characterization.

3.4. General characterization

Surface area and other associated textural properties (like porosity, pore size, volume and surface specific area (SSA)) of the synthesized sample were detected by using the method of N_2adsorption-desorption measurements at 77K, using Quantachrome Nova-Win (©1994-2018, version 11.05).For calculating the SSA, size and volume of pore, BET method and BJH methods were applied. Samples were degassed for 90 minutes at 200°C and 500 mm Hg. t-plot method was used for finding micropore volume. Mesopore volume was measured through the below relation.

$$V_{(meso)}\ (cm^3g^{-1}) = V_{(total)} - V_{(micro)} \quad \text{---------- (1)}$$

Data for specific surface area calculation was collected using p/p_0 values ranging from 0.05 to 0.95. In these calculations we can find accurate results for pores having diameter larger than 4nm.

To investigate thermal stability, weight loss of the material during the processes of carbonization and activation, thermal gravimetric analysis was conducted under inert gas environment of Nitrogen within the temperature range of 25°C to 750°C with 10°C/min ramp on TGA 5500 of TA instruments. To review the crystal structure of the synthesized algae derived activated carbon, XRD analysis was conducted using DRON-8 (pXRD)instrument, in the 2 theta (2 θ) scale ranging from 15° to 55° with a radiation source of Cu-Kα (Kα=1.5418Å).

Raman spectroscopy was conducted using BTC162E-532S-SYS [USA] system at 531.82 nm laser wavelength to investigate the vibrational response of the sample. Using Cary 630 FTIR (Agilent Technologies, USA), FTIR spectroscopy was conducted to detect functional groups and to detect information related to physical state and chemical composition of the sample. Information about surface morphology (textural characterization) and elemental analysis of algal biomass, carbonized sample and Spy-AC-750 were collected from the images and graphs captured by SEM (Oxford Instruments, UK).

3.5. Electrode preparation and symmetric cell fabrication

Polyvinylidene-Fluoride (PVDF) (as binder), carbon black and one of the synthesized Spy-AC from Spy-AC-700, Spy-AC-750, Spy-AC-800 and Spy-AC-850 (as active material) were assorted in the ratio by weight of 10%, 10% and 80% respectively to form a slurry for coating on working electrode to analyze the performance of the Spy-ACs as an electrode material. Then the prepared slurry was loaded on the surface of the nickel foam and placed in an oven to dry at 85°C for 180 minutes. Each electrode of symmetric cell was coated with 1 mg cm^{-2} of the Spy-AC-750 followed by vacuum drying. 1 M KOH electrolyte was used between the two electrodes separated by a separator.

3.6. Electrochemical characterizations

Using CHI760E electrochemical workstation, this study evaluates the electrochemical behavior of the Spy-ACs deposited electrode in three electrode configurations. For measuring the performance of single electrode, 3M KOH solution as electrolyte, a working electrode made of the Spy-AC deposited on nickel foam, a counter electrode of platinum

wire and reference electrode of Ag/AgCl was used in the electrochemical work station. Cyclic voltammetry (CV), Galvanostatic Charge Discharge (GCD) and Electrochemical Impedance Spectroscopy (EIS) were conducted for investigating the electrochemical characteristics of the Spy-AC-750 coated electrodes. CV curves were recorded at various scan rates from 5 to 100 mV/s between the potential range -0.2 to 0.2 V. GCD curves of the electrodes were recorded at various current densities ranging from 0.5 to 2.5 A/g. EIS spectra were detected at 100 kHz to 0.100 Hz frequency. By using the below relations with data from the GCD curves, gravimetric specific capacitance i.e. Cm, (F/g), Energy density E (Wh/kg) and Power density P (W/kg) can be calculated.

$$Cm = (I \times \Delta t) / (m \times \Delta V) \text{----------(2)}$$

$$E = (0.5 \times Cm)(\Delta V^2/3.6) \text{----------(3)}$$

$$P = (3600 \times E/\Delta t) \text{----------(4)}$$

Cm: Specific capacitance of the material used in electrodes (F/g)

I: Discharge Current (A)

Δt: Time (sec)

ΔV: Mass of the active material of electrode (g)

Summary

This chapter explained the various steps adopted for the synthesis of activated carbon using *Spirogyra* algae as a precursor. These steps include collection of algae, sun-drying, pulverization, carbonization, addition of an activation agent, activation, washing, drying, and storing. During this experimental methodology, various equipment and chemicals have been used to prepare activated carbon. The experiments for the preparation of activated carbon have been conducted at the Biofuel lab, the Energy Storage Lab, and the Advanced Energy material synthesis Lab at USPCAS-E, NUST. After synthesis and activation, the different samples of the activated carbon were tested for morphological and electrochemical characterizations.

References

[01] A. El-Sikaily, A. El Nemr, and A. Khaled, "Copper sorption onto dried red alga Pterocladia capillacea and its activated carbon," *Chem. Eng. J.*, vol. 168, no. 2, pp. 707–714, 2011, doi: https://doi.org/10.1016/j.cej.2011.01.064.

[02] H. J. Cho, K. Baek, J. K. Jeon, S. H. Park, D. J. Suh, and Y. K. Park, "Removal characteristics of copper by marine macro-algae-derived chars," *Chem. Eng. J.*, vol. 217, pp. 205–211, 2013, doi: 10.1016/j.cej.2012.11.123.

[03] Y. M. Chang, W. T. Tsai, M. H. Li, and S. H. Chang, "Preparation and characterization of porous carbon material from post-extracted algal residue by a thermogravimetric system," *Algal Res.*, vol. 9, pp. 8–13, 2015, doi: 10.1016/j.algal.2015.02.011.

[04] Y. M. Chang, W. T. Tsai, and M. H. Li, "Characterization of activated carbon prepared from chlorella-based algal residue," *Bioresour. Technol.*, vol. 184, pp. 344–348, May 2015, doi: 10.1016/j.biortech.2014.09.131.

[05] A. Salima, B. Benaouda, B. Noureddine, and L. Duclaux, "Application of Ulva lactuca and Systoceira stricta algae-based activated carbons to hazardous cationic dyes removal from industrial effluents," *Water Res.*, vol. 47, no. 10, pp. 3375–3388, 2013, doi: https://doi.org/10.1016/j.watres.2013.03.038.

[06] M. Kılıç, E. Apaydın-Varol, and A. E. Pütün, "Preparation and surface characterization of activated carbons from Euphorbia rigida by chemical activation with ZnCl2, K2CO3, NaOH and H3PO4," *Appl. Surf. Sci.*, vol. 261, pp. 247–254, 2012, doi: https://doi.org/10.1016/j.apsusc.2012.07.155.

[07] M. Wang, F. Hao, G. Li, J. Huang, N. Bao, and L. Huang, "Preparation of Enteromorpha prolifera-based cetyl trimethyl ammonium bromide-doped activated carbon and its application for nickel(II) removal," *Ecotoxicol. Environ. Saf.*, vol. 104, pp. 254–262, 2014, doi: https://doi.org/10.1016/j.ecoenv.2014.01.038.

[08] M. Sevilla, W. Gu, C. Falco, M. M. Titirici, A. B. Fuertes, and G. Yushin, "Hydrothermal synthesis of microalgae-derived microporous carbons for electrochemical capacitors," *J. Power Sources*, vol. 267, pp. 26–32, 2014, doi: https://doi.org/10.1016/j.jpowsour.2014.05.046.

[09] E. Elaiyappillai *et al.*, "Low cost activated carbon derived from Cucumis melo fruit peel for electrochemical supercapacitor application," *Appl. Surf. Sci.*, vol. 486, pp. 527–538, Aug. 2019, doi: 10.1016/j.apsusc.2019.05.004.

[10] S. Altenor, M. C. Ncibi, E. Emmanuel, and S. Gaspard, "Textural characteristics, physiochemical properties and adsorption efficiencies of Caribbean alga Turbinaria turbinata and its derived carbonaceous materials for water treatment application," *Biochem. Eng. J.*, vol. 67, pp. 35–44, 2012, doi: https://doi.org/10.1016/j.bej.2012.05.008.

[11] H. P. S. Abdul Khalil *et al.*, "Biodegradable polymer films from seaweed

polysaccharides: A review on cellulose as a reinforcement material," *Express Polym. Lett.*, vol. 11, no. 4, pp. 244–265, 2017, doi: 10.3144/expresspolymlett.2017.26.

[12] B. F. Sviridenko, T. V. Sviridenko, and K. S. Yevzhenko, "Discovery of *Spirogyra* subcolligata Bi (*Spirogyra*ceae, Zygnematales) in Russia," *Inl. Water Biol.*, vol. 8, no. 3, pp. 218–221, 2015, doi: 10.1134/S199508291503013X

[13] A. Jain, R. Balasubramanian, M.P. Srinivasan, Hydrothermal Conversion of Biomass Waste to Activated Carbon with High Porosity: A Review Hydrothermal conversion of biomass waste to activated carbon with high porosity: A review, Chem. Eng. J. 283 (2015) 789–805. doi: 10.1016/j.cej.2015.08.014.

[14] G.K. Parshetti, S. Chowdhury, R. Balasubramanian, Biomass derived low-cost microporous adsorbents for efficient CO2 capture, Fuel. 148 (2015) 246–254. doi: 10.1016/j.fuel.2015.01.032.

[15] M.G. Plaza, C. Pevida, C.F. Martín, J. Fermoso, J.J. Pis, F. Rubiera, Developing almond shell-derived activated carbons as CO2 adsorbents, Sep. Purif. Technol. 71 (2010) 102–106. doi: 10.1016/j.seppur.2009.11.008.

[16] M. Li, R. Xiao, Preparation of a dual Pore Structure Activated Carbon from Rice Husk Char as an Adsorbent for CO2 Capture, Fuel Process. Technol. 186 (2019) 35–39. doi: 10.1016/j.fuproc.2018.12.015.

[17] S.G. Herawan, M.S. Hadi, M.R. Ayob, A. Putra, Characterization of activated carbons from oil-palm shell by CO2 activation with no holding carbonization temperature, Sci. World J. 2013 (2013). doi:10.1155/2013/624865.

[18] P.H. Huang, H.H. Cheng, S.H. Lin, Adsorption of carbon dioxide onto activated carbon prepared from coconut shells, J. Chem. 2015 (2015). doi:10.1155/2015/106590.

Chapter 4

Results and discussion

4.1. Morphological Analysis

Spirogyra derived activated carbon stepwise preparation including carbonization and activation is shown schematically in Fig. 3.1. During activation at temperatures higher than 700°C the probable chemical reactions are given below[1][2].

$$6\ KOH + 2\ C \longrightarrow 2\ K + 2\ K_2CO_3 + 3\ H_2 \quad (4.1)$$

$$K_2CO_3 \longrightarrow K_2O + CO_2 \quad (4.2)$$

$$CO_2 + C \longrightarrow 2\ CO \quad (4.3)$$

$$K_2CO_3 + 2\ C \longrightarrow 2\ K + 3\ CO \quad (4.4)$$

$$K_2O + C \longrightarrow 2\ K + CO \quad (4.5)$$

4.1.1. Surface analysis using Scanning Electron Microscope (SEM)

Textural morphologies of the surface of *Spirogyra* algae, carbonized sample and Spy-AC-750 analyzed by SEM. Images captured at different magnifications are shown in Fig. 4.1.
Fig. 4.1 (a), (b), and (c) shows surface structure of dried powder of *Spirogyra* algae. Fig. 4.1 (d), (e), and (f) shows surface structure of carbonized sample having compact and crude structure with limited porosity. And Fig. 4.1 (g), (h), and (i) represents textural surface structures with porosity and enhanced surface area of the Spy-AC-750 activated at 750°C. From the surface structure of Spy-AC-750 it can be concluded that KOH is acting as a pore forming agent and hence enhances surface area and porosity [3]. KOH as activation agent in the process of activation, at 400°C reacts with C and produces K_2CO_3 as shown in the reaction (Equation 4.1). During this reaction partial consumption of carbon results the formation of pores. Almost complete consumption of KOH takes place with the rising of temperature up to 600°C. At 700°C, CO_2 and K_2O formation take place due to the decomposition of K_2CO_3 (Equation 4.2). At this K_2CO_3 decomposition stage, pore formation also takes place. At high temperature stage (700°C and above), the resultant CO_2 reduces to CO while reacting with more carbon at high temperature (Equation 4.3). More reduction reactions of K_2CO_3 and K_2O take place resulting in carbon mono oxide and metallic K (Equations 4.4 & 4.5).

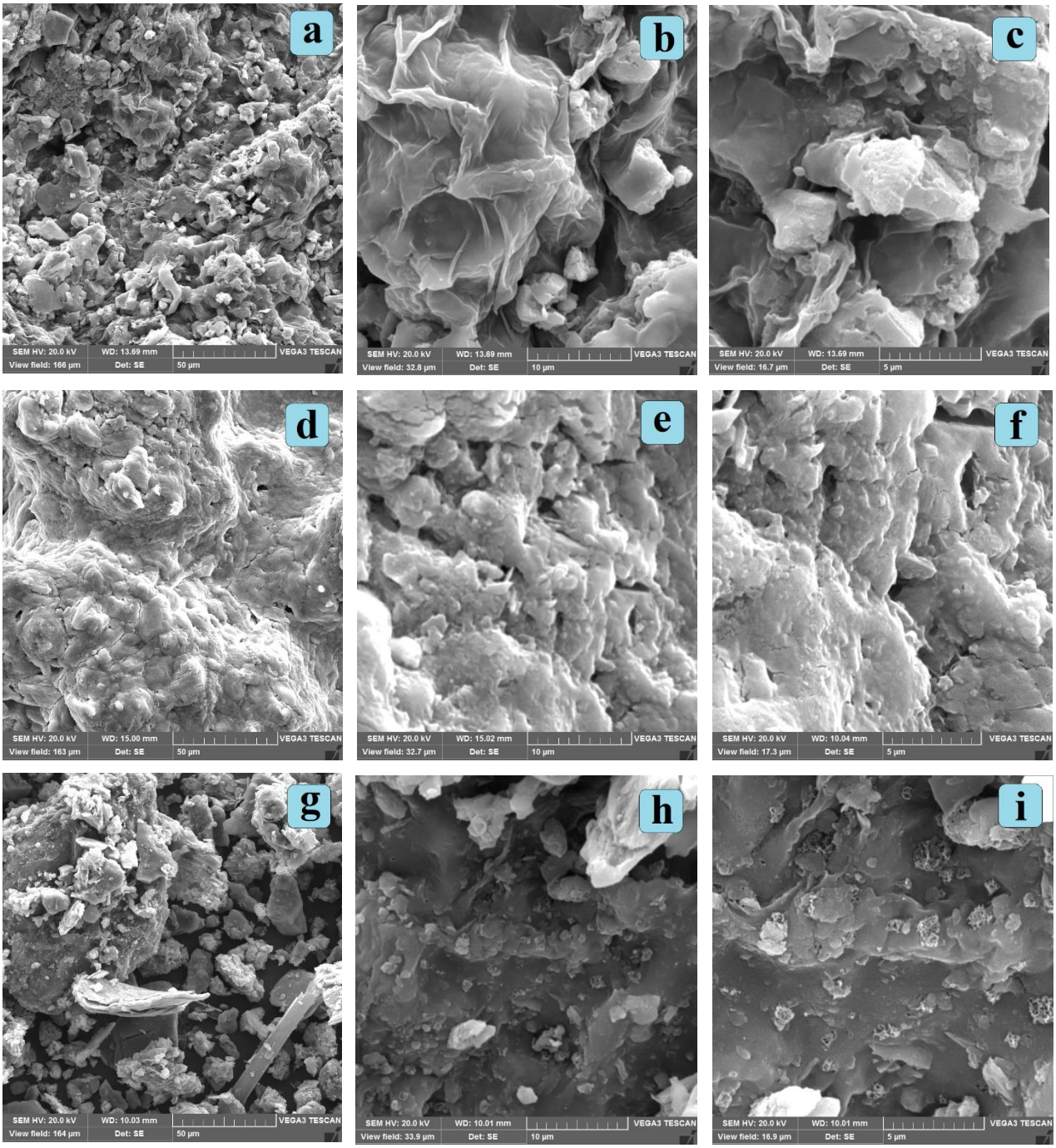

Figure 4-1: SEM images of algal biomass (at (a) 50 µm, (b) 10 µm, (c) 5µm), carbonized sample (at (d) 50 µm, (e) 10 µm, (f) 5µm) and Spy-AC-750 (at (g) 50 µm, (h) 10 µm, (i) 5µm)

At high temperature during these two reaction stages (Equations 4.4 & 4.5) products diffuse into the carbon resulting the enhancement in the porosity of the carbon [3][4][5]. When activated carbon (porous) is used as electrode material in supercapacitors, due to pores on the surface of electrode, there is a remarkable boost in diffusion of mobile ions take place. Porosity also causes to shorten the path of the diffusion for mobile ions [6]. Enhanced

porosity of Spy-AC-750 causes an astonishing increase in charge storage ability of supercapacitors[7].

EDS analysis of the surface of algae and activated carbon (Spy-AC-750) indicate the presence of carbon content and other ignorable elements as shown in Fig. 4.2. The results of EDS analysis were calculated by using the average and mean value of all obtained values from different points of the samples. This analysis also shows that at 750°C purer AC has been achieved.

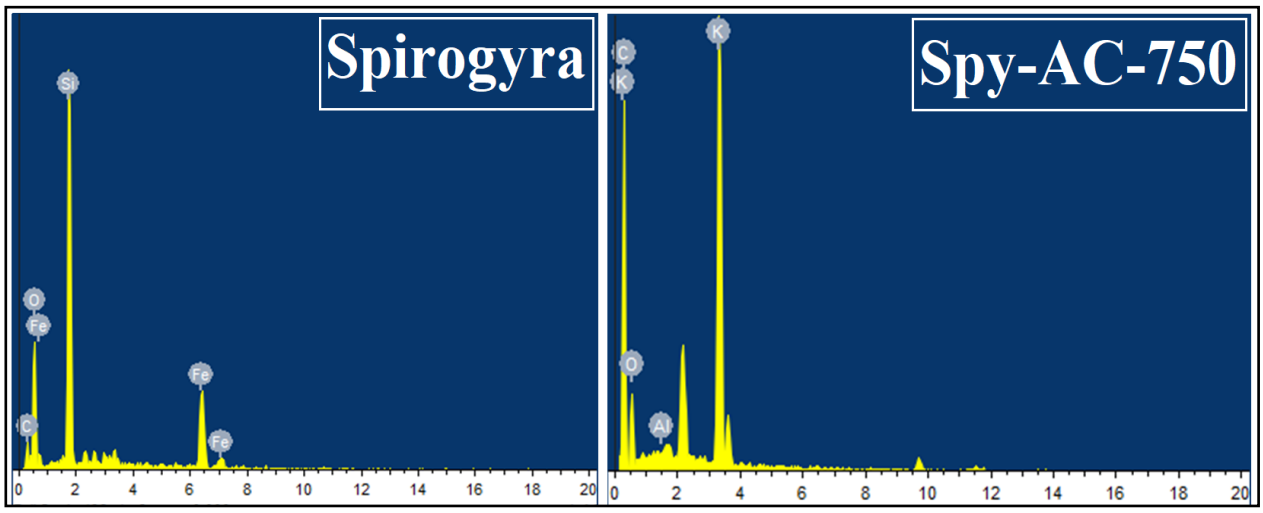

Fig. 4-2: EDS Analysis of *Spirogyra* and Spy-AC-750

4.1.2. Thermo-gravimetric Analysis

TGA was conducted to study the sample's weight loss and thermal stability during the carbonization and activation stages as shown in Fig.4.3. The TGA plot shows that biomass decomposition takes place at 25 to 260°C, resulting 11 % weight loss and the temperature peak at 289 correlates to evaporation of water content (dehydration). A large percentage of weight loss (69%) was recorded in the second step from 260 to 395°C. This loss is ascribed to the release of CO_2 molecules and biomass decomposition. While heating the sample from 395 to 610°C, due to high temperature pyrolysis, a weight loss of 15% was recorded [8][9]. Beyond 610 to 750°C no weight loss was recorded, expressing that the presence of carbon is about 4 to 5 percent in the *Spirogyra* specie.

While in case of pure Spy-AC-750, a weight loss of only up-to 20% was observed from 25°C to 750°C with a ramp rate of 10°C /minute expressing purity and stable nature of the Spy-AC-750.

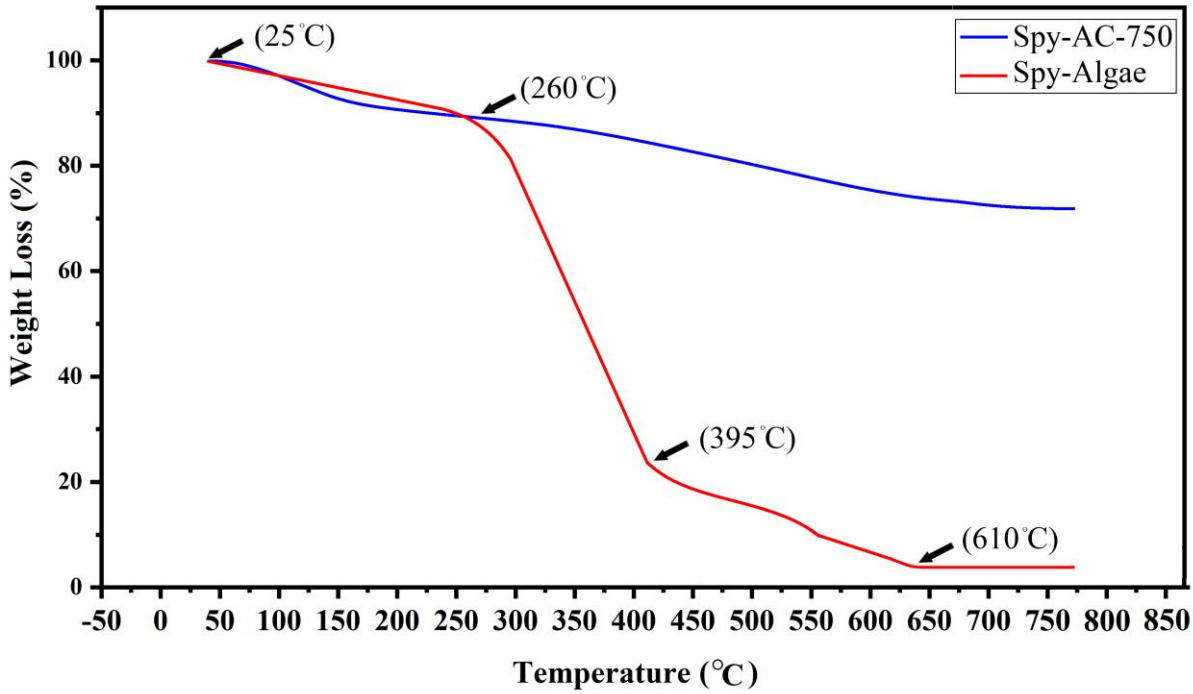

Fig. 4-3: Thermo-gravimetric Analysis of Spy-AC 750

4.1.3. XRD

The crystal structure characterization of Spy-AC-750 at micro level was reviewed by XRD patterns. In the XRD spectrum, peaks with high intensity reveals that there is superior crystallinity in the carbon structure and hence showing higher diffraction in the graph. Higher the crystallinity in the carbon structure, higher will be the diffraction in the XRD pattern. In Fig. 4.4, the pattern is composed of two distinct diffraction peaks at 23.6° and 43.1°. The peak at 23.6° is attributed to carbon (002) reflections, showing a low degree of graphitization and crystalline nature[10], while the peak at 43.1° is attributed to (100) reflections indicating disordered nature of the carbon [11].

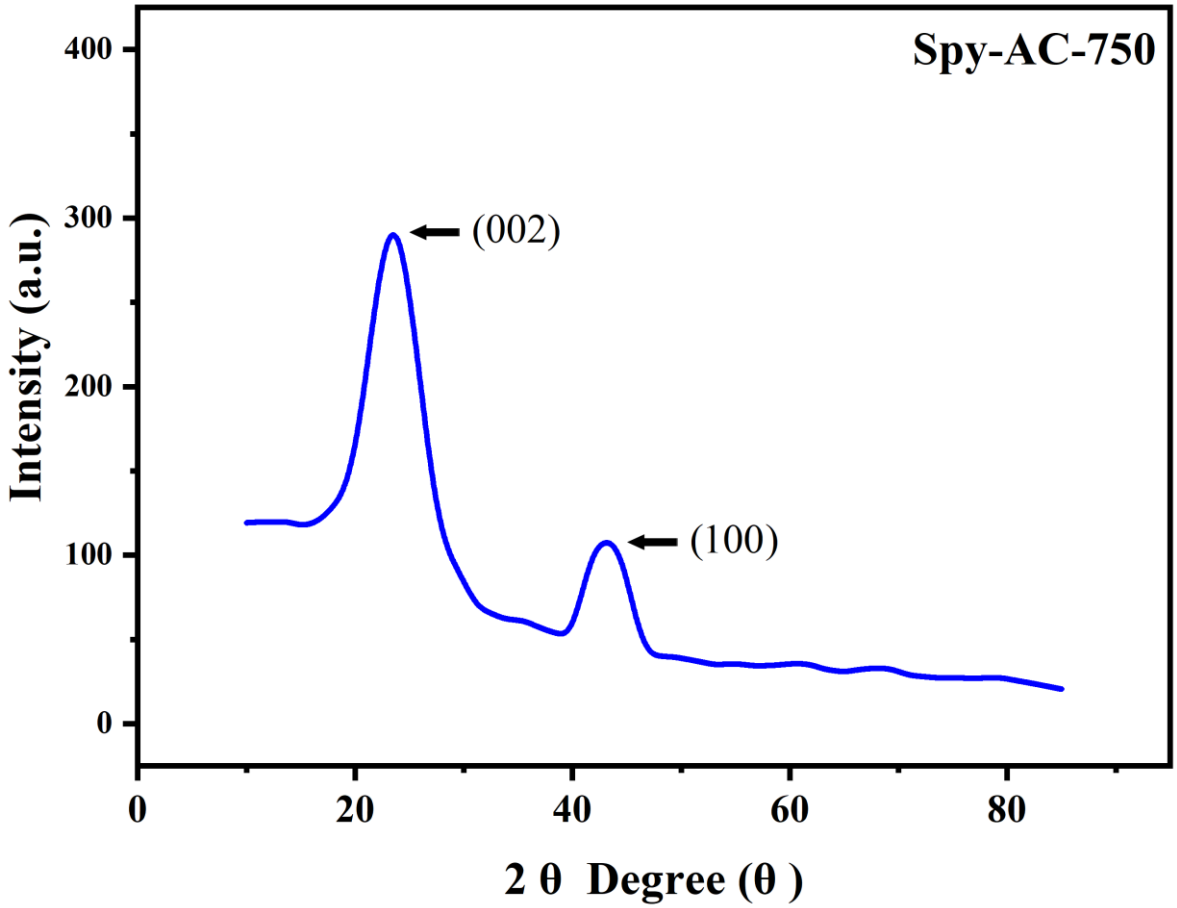

Fig. 4-4: XRD spectrum of Spy-AC-750

4.1.4. FTIR

Presence of various functional groups in the Spy AC-750 was detected through FTIR spectrum (Cary 630 FTIR, Agilent Technologies, USA) using standard procedure. Carbon materials' FTIR spectra are prone to inherent aberrations, making data interpretation difficult [12]. In the wavenumber range of 500–4000 per cm, FTIR spectra of the Spy AC-750, indicating the presence of hydroxyl, carboxyl, and carbonyl groups (O_2comprising functional groups) as shown in Fig. 4.5.

Different peak points at 3300 cm^{-1} and 1570 $cm^{-1}$are refer to carbonyl group (C=O) and Hydroxyl group (-OH) bond stretching in carboxyl groups. The peak at 1002$cm^{-1}$is assigned to C-O stretching [13][14]. At 2316 and 2095 cm^{-1} peak points refers to the presence of C-O and C≡C bonds in ketene and alkyne groups. And the peak at 728$cm^{-1}$is assigned for the presence of ethane groups [15]. The existence of oxygen in C-O bonds could be found in different surface functional groups. Phenols, anhydrides, carboxyl, and lactones are acidic O_2-containg functional groups. Chromene, pyrone, and quinone are basic oxygen containing functional groups, while ether and carbonyl are neutral groups [14]. Carbon surface

wettability may be enhanced by the presence of acidic and basic O_2-containing functional groups. But existence of these groups may also lower the electronic conductivity of the carbon surface. These functional groups in activated carbon could also increase the property of self-discharge in supercapacitors' electrode by the decomposition of electrolyte material and by catalyzing carbon oxidation and reduction [16][17].

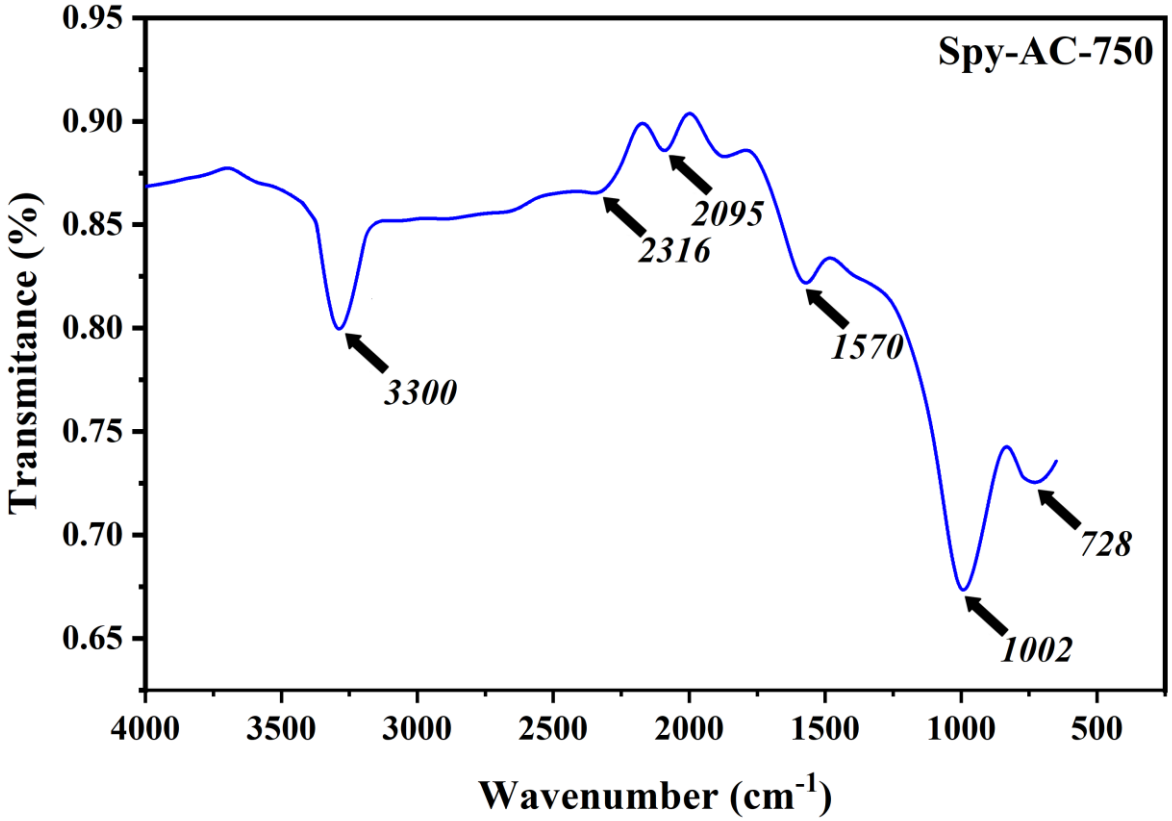

Fig. 4-5: FTIR spectrum of Spy-AC-750

4.1.5. Raman Spectroscopy

To investigate the structural features like stability and vibrational response of Spy-AC-750, Raman spectroscopy was applied at 531.82nm laser wavelength.

Two intense bands at 1331 cm^{-1} and at 1565 cm^{-1} corresponds to "D" (diamond) and "G" (graphite) phases of the activated carbon are shown in Fig. 4.6. Disordered microcrystalline domain of the sp^2 bonded carbon atoms comprised in the vibrational modes. The D-band in the graph at 1331 cm^{-1} is assigned to the point phonons' breathing mode. This mode resembles to the disorganized form or defective-graphitic-structure of the carbon [18]. While G band in the graph at 1565 cm^{-1} indicates the symmetric C-C vibrations of the sp^2 hybridized carbon graphitic structure [8][19][20]. Fig. 4.6 shows that the intensity (I_G) at G band is a little bit higher than the intensity (I_D) at D band, indicating the finer structure due

to activation by KOH. Typically, the value of I_G/I_D describes the graphitic property of activated carbon[21]. Here the value of I_G/I_D ratio of Spy-AC-750 is 0.995, indicating high conductivity and high graphitization of the synthesized material. Carbon with high graphitic and conductive nature leads to high capacity for charge storage [21].

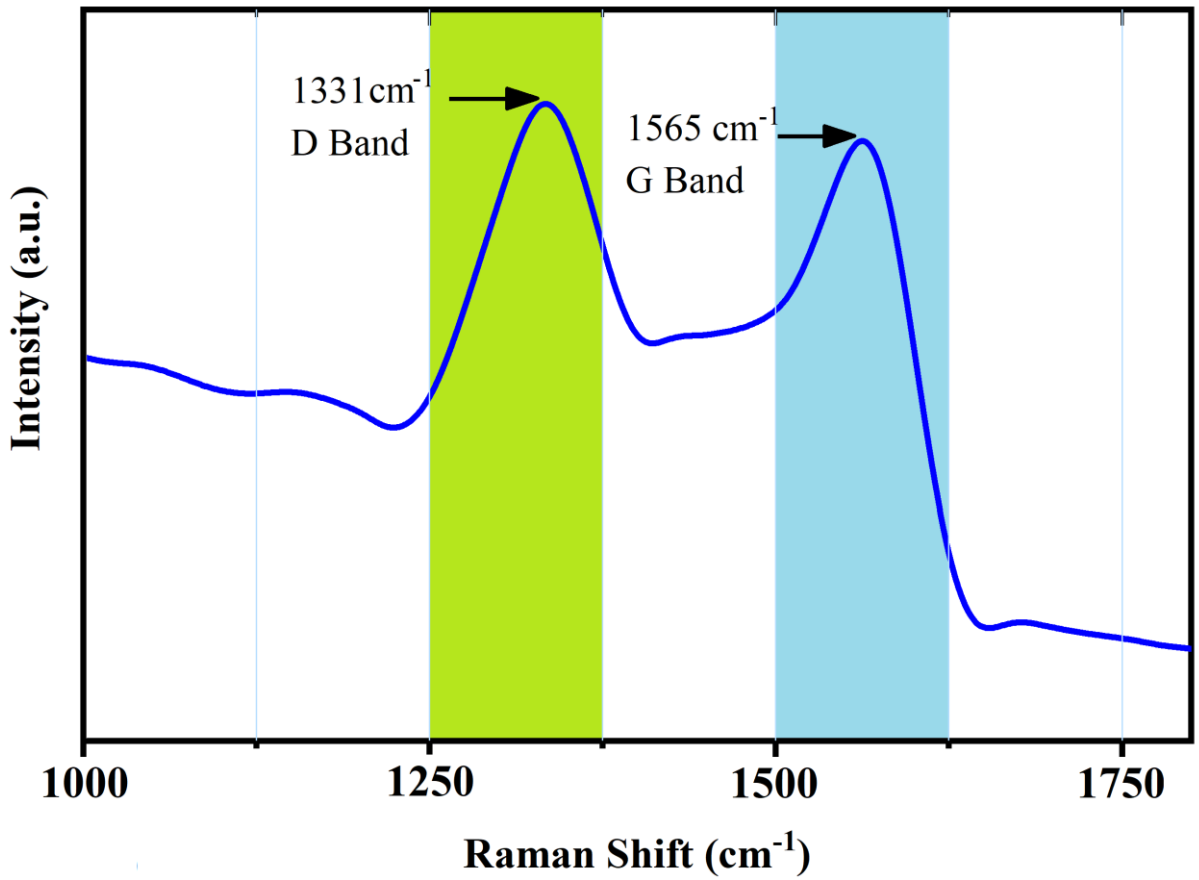

Fig. 4-6: Raman Spectroscopy of Spy-AC-750

4.1.6. N_2 adsorption desorption isotherm, surface area analysis

The BET method and pore size distributions are the two basic approaches used to characterize the porous structures of activated carbon. In Fig. 4.7, the results of N_2 adsorption desorption isotherms analyzed at 77K showing the presence of micro-porosity as well as meso-porosity in the surface of Spy-AC-750 because of increasing N_2 adsorption at relatively low pressure [22].The hysteresis loop (at P/P_0 >0.45) between the adsorption and desorption branches of the isotherms, indicates the coexistence of mesopores and micropores, especially when activation was performed by the use of KOH. Table 4-1 shows the textural features of the Spy-AC-750.

Table-4.1: Textural morphology of Spy-AC-750

Sample	BET SSA (m^2/g)	Area of micropore (m^2/g)	Total Pore Vol. (cm^3/g)	Pore Diameter (nm)
Spy-AC-750	727.765 m^2/g	611	0.317	1.23

Table 4-2 shows the comparison of BET specific surface area (SSA) of Spy-AC-750 with the SSA of different biomass derived activated carbons. From the literature it is clear that the SSA is concerned with final activation temperature as shown in Table 2.

Table 4-2: Comparison of Textural and surface properties Biomass derived AC with Spy-AC-750

Biomass	**Activation Temp (°C)**	**S_{BET} (m^2/g)**	**Total Vol. (cm^3/g)**	**Pore radius (nm)**	**References**
Coir Pith	700	910	0.363	0.8	[23]
Char of tyre	750	700	1.099	-	[24]
Chestnut Shells	850	590.8	0.32	-	[25]
Perilla Frutescens	800	712	0.56	-	[26]
Neem Leaves	800	705	0.44	2.5	[27]
Coffee Residue	600	890	077	3.5	[28]
Spy-AC-750	750	727	0.317	0.65	(This Study)

Results confirm that KOH activation and high temperature of activation are the two basic factors for enhancing the SSA of the activated carbon. Due to enhanced SSA, movement of electrolyte ions and electrons will be faster and hence electrochemical performance of supercapacitor will be enhanced [29][30]. Using BET method, SSA of Spy-AC-750 was calculated as 727.765 m^2/g.

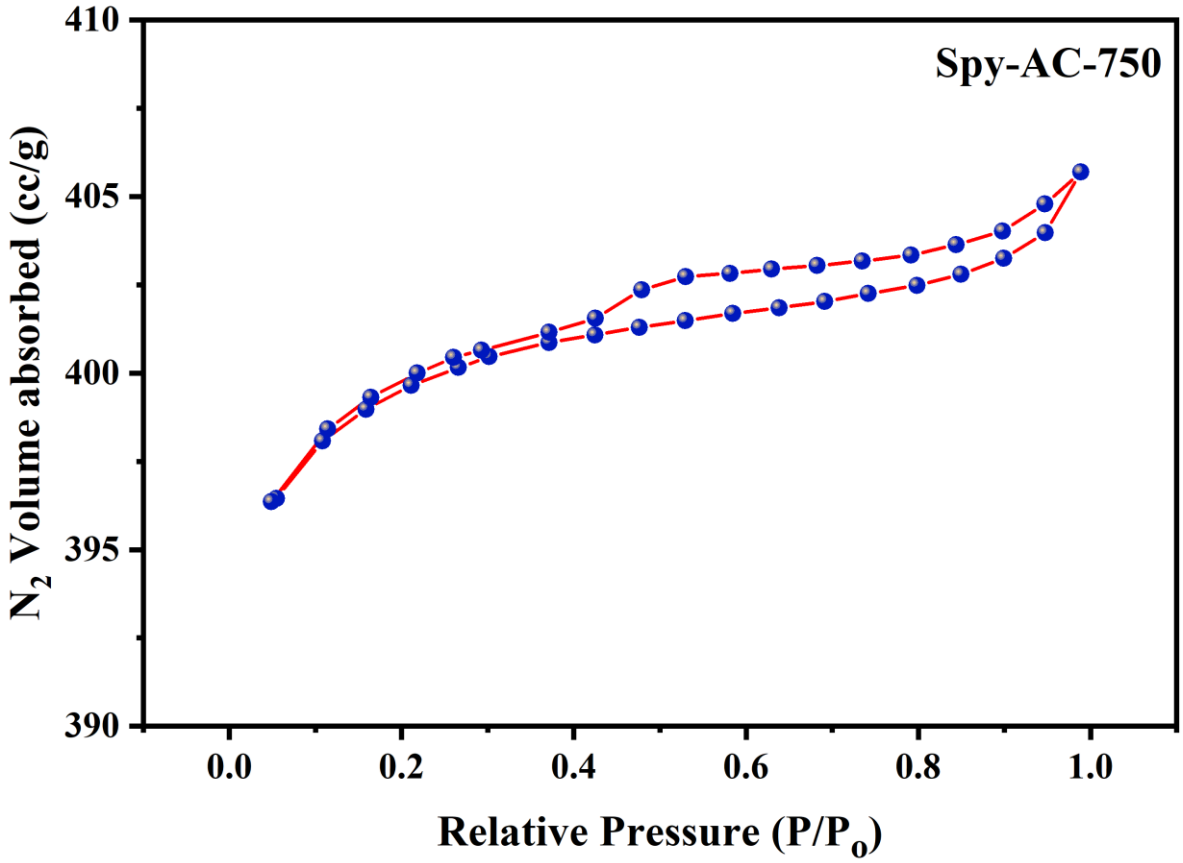

Fig. 4-7: N2 adsorption desorption isotherm of Spy-AC-750

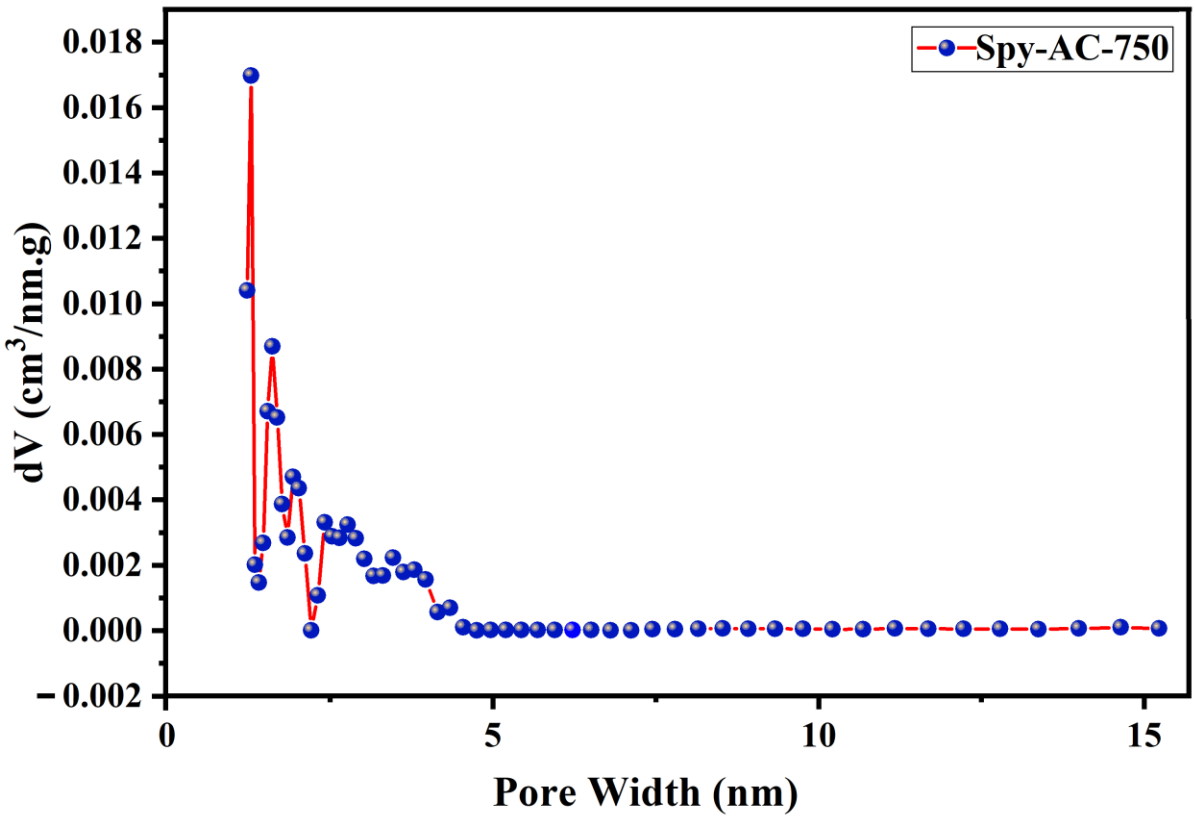

Fig. 4-8: Pore size distribution of Spy-AC-750

BJH method was used to analyze pore size distribution as depicted in Fig. 4.8. Spy-AC-750 is providing a hierarchical porous morphology with micro and mesopores having average size of 3.50 to 4.40 nm. Spy-AC-750 shows the presence of highest micropore distribution with remarkable absorption volume. Fig.4.8 clarifies that Spy-AC-750 has isotherm of type I and type IV as per classification of IUPAC, expressing much amount of mesopores and micropores in the surface of Spy-AC-750 [31]. KOH has significantly enhanced hierarchical 3D porous structure with micro-meso porosity which is considered as more effective electrode material for the fabrication of supercapacitors [32]. Micropores lead to the formation of many electric double layers by providing a large surface area, whereas mesopores provide a very broad ion transfer mechanism. The combination of these two characteristics boosts the use of porous activated carbon for electrochemical energy storage devices.

4.2. Electrochemical Characterizations Results

4.2.1. Cyclic Voltammetric (CV) Tests

The Electrochemical performance of *Spirogyra* Algae derived AC prepared at different temperatures (700°C, 750°C, 800°C and 850°C) named as AC-700, Spy-AC-750, AC-800 and AC-850 has been compared in a three-electrode system at a scan rate of 100 mV/s with a voltage range of -0.2 to 0.2 V in an electrolyte of 3M KOH solution using CHI760E electrochemical workstation. Curves of the CV are shown in Fig. 4.9.The Curve of Spy-AC-750 has a quasi-rectangular like shape as compared to the remaining three types of ACs. Rectangular shape may express several factors like channels for rapid transport of ions inside mesopores, low distance of electrolyte diffusion within micropores for ion desorption between micro and mesopores [10]. In addition, closed area of CV curve shows that Spy-AC-750 has a high specific capacitance of 206.5 F/g. Due to this reason this study is mainly focuses on the characteristics of Spy-AC-750. Fig. 4.10 expresses the electrochemical behavior of Spy-AC-750 at various scan rates ranging from 5.0mVs^{-1} to 100 mVs^{-1}. The curve shape of CV remains the same even at high scan rate with no redox peaks in the curve, expressing the capacitive characteristic of the AC and also the process of charge storage occur due to adsorption-desorption mechanism [33][34][37]. When compared to the CV data of other biomass-derived activated carbons, Spy-AC-750 confirms that it is an appropriate electrode material for electrochemical energy storage devices.

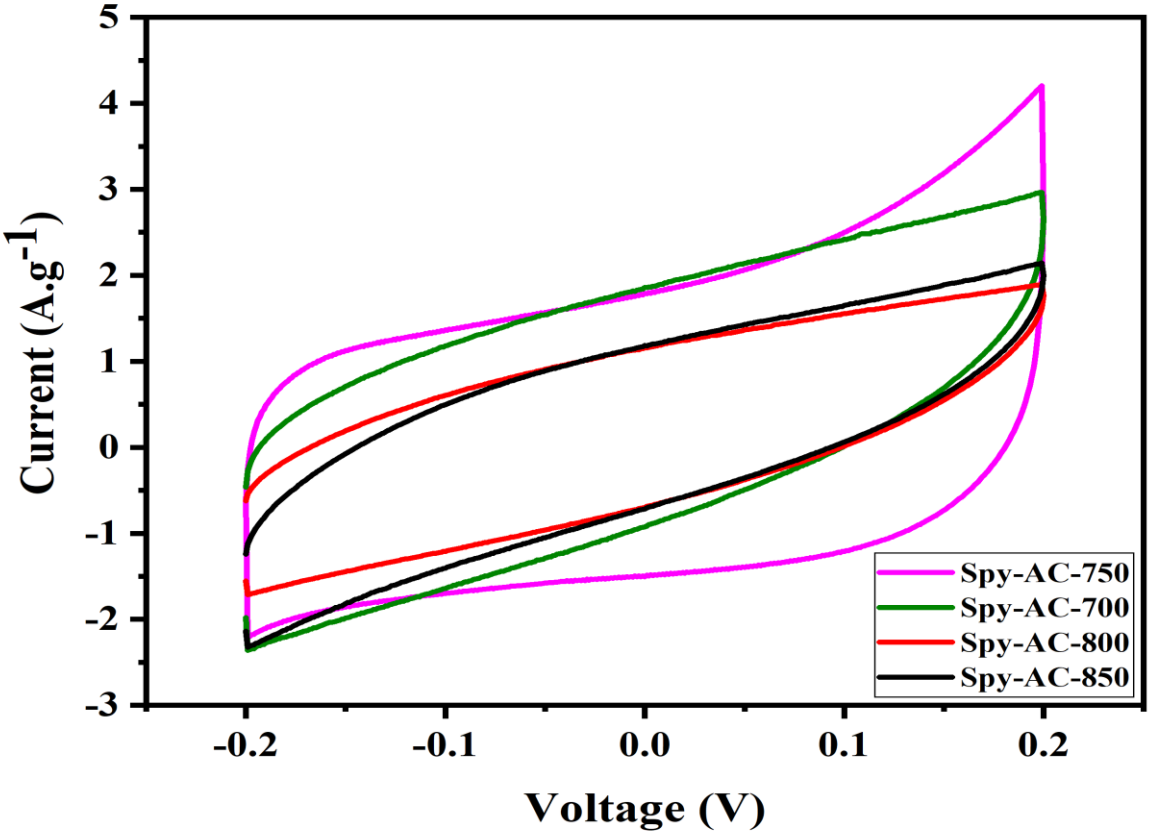

Fig. 4-9: Cyclic Voltammetry of Spy-AC-700, Spy-AC-750, Spy-AC-800 and Spy-AC-850

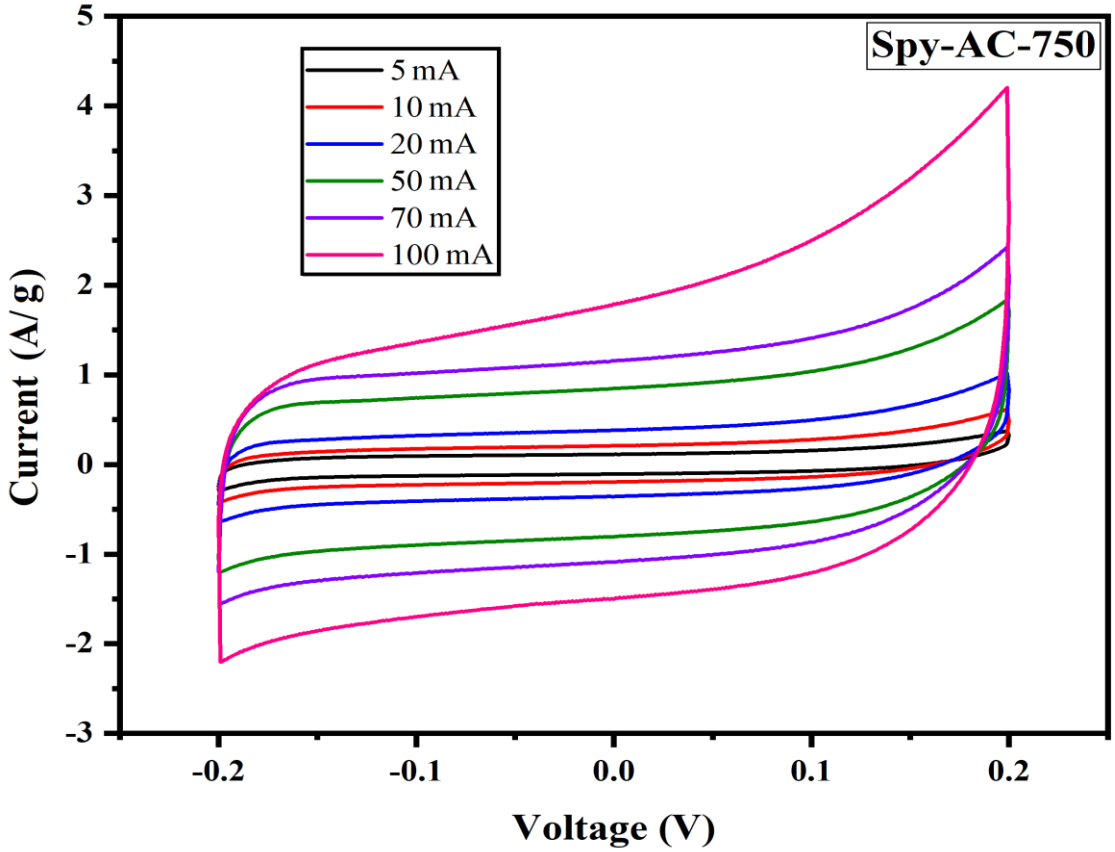

Fig. 4-10: CV of Spy-AC-750 at various scan rates

4.2.2. Galvanostatic Charging-Discharging (GCD) Tests:

The charge capacitance of the material used in the electrodes of storage devices is determined through GCD testing. Comparison of GCD results of Spy-AC-700, Spy-AC-750, Spy-AC-800, and Spy-AC-850 at 0.5 A/g scan rate is shown in Fig. 4.11.GCD curves of Spy-AC-750 maintained an isosceles triangle with zero deformation at 100A/g scan rate showing the behavior of EDLC capacitors [35].

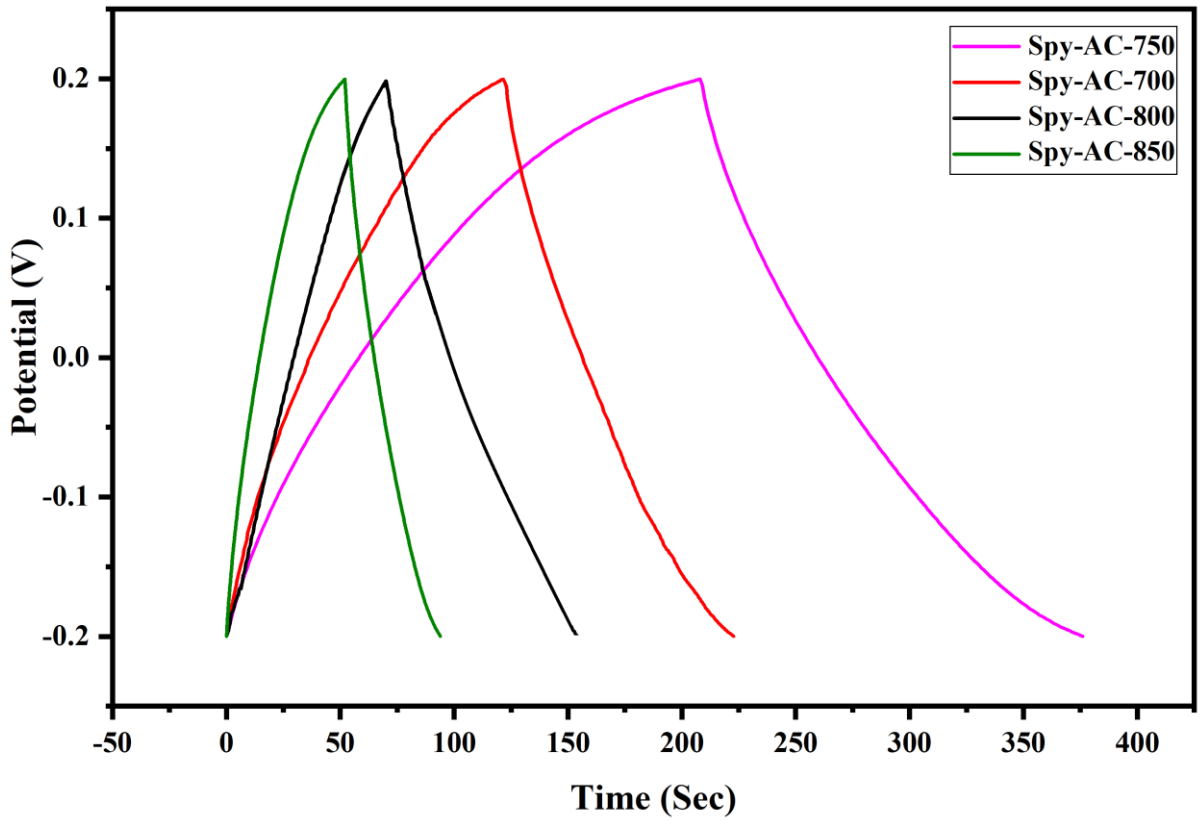

Fig. 4-11: Comparison of GCD results of Spy-AC-700, Spy-AC-750, Spy-AC-800, and Spy-AC-850

GCD curves of Spy-AC-750 at various scan rates within a voltage range of -0.2 to 0.2 V are shown in Fig. 4.12. Curve analysis exhibits a comparatively reasonable time of charging and discharging with excellent specific capacity storage. The GCD plots of the Spy-AC-750 applied electrode exhibits quasi-isosceles triangular shape, with low V (IR) drops showing good coulumbic efficiency with low series resistance, suggesting EDLC nature [33]. At a current density of 0.5 Ag^{-1}, the Spy-AC-750 applied electrode has a high specific capacitance of 210 Fg^{-1}.

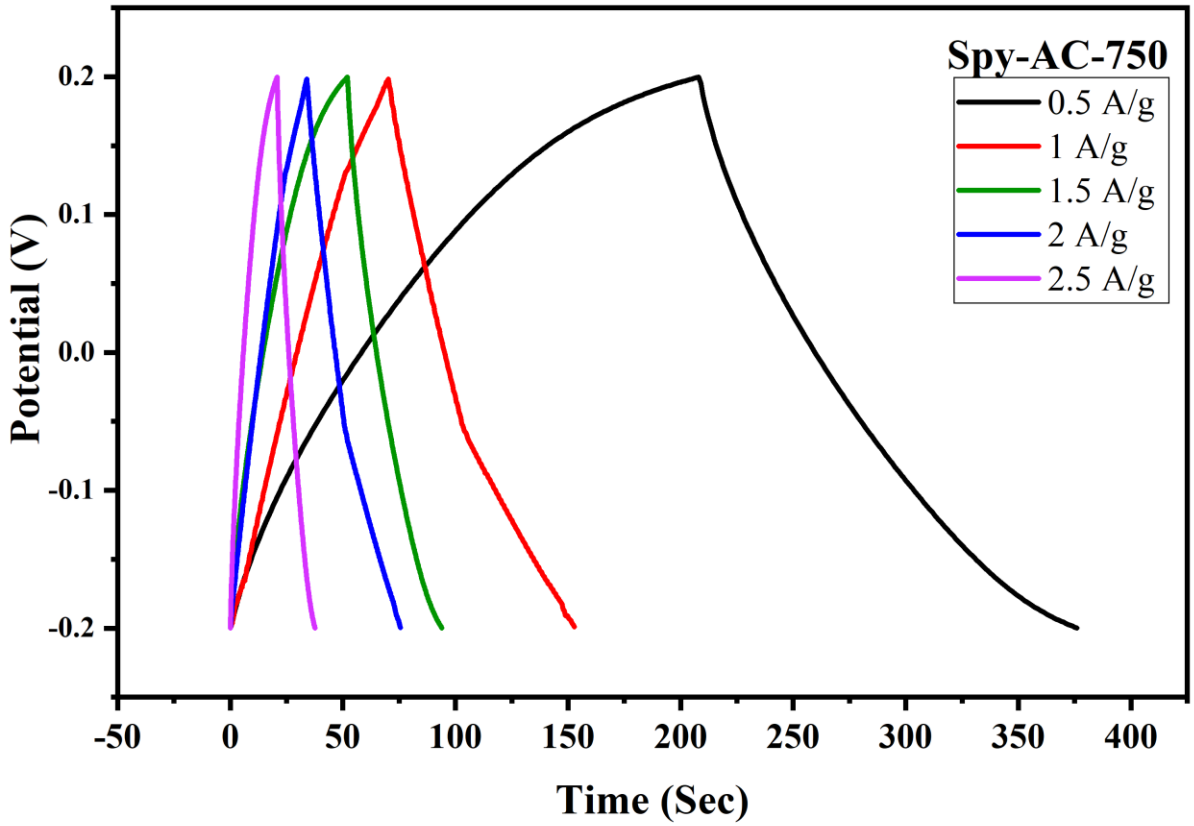

Fig. 4-12: GCD Curve of Spy-AC-750 at various scan rates

4.2.3. Electrochemical Impedance Spectroscopic (EIS) Analysis

To identify and assess the electrochemical conductivity and resistance of the electrode, an EIS study was performed at a frequency range of 100.00 kHz – 0.01 Hz. The Nyquist curves for Spy-AC-700, Spy-AC-750, Spy-AC-800 and Spy-AC-850 applied electrodes are depicted in Fig. 4.13. Fig. 4.13 clarifies that only Spy-AC-750 show short intercept (less than 0.650) expressing remarkable power capability as well as low equivalent series resistance [35]. "Niquist plot of Spy-AC-750 is shown in Fig. 4.14 indicating that at high frequency, a semicircle travels across a straight line in the low frequency zone. The value of resistance in series (R_s) is plotted in Nyquist plot (comprising the material intrinsic resistance, electrolyte resistance and contact resistance of current collector and electrode). The presence of resistance during charge transfer (R_{ct}) is shown by the semicircle-like shape in the Nyquist plot (inset plot in Fig. 4.14) , and its presence at high frequency is mostly due to porosity in the electrode, interfacial contact, and inter-partial contact of current collector and electrode[36]. R_w is the Warburg diffusion resistance existing in the Nyquist plots at low frequency region. Comparing with other electrode materials,Spy-AC-750 shows lower values of R_{ct} and R_s. In Nyquist plot, Spy-AC-750 electrode material

represents segments of vertical line and semicircle at low and high frequency regions respectively, expressing that Spy-AC-750 has a promising capacitive and ideal wettability nature [33].

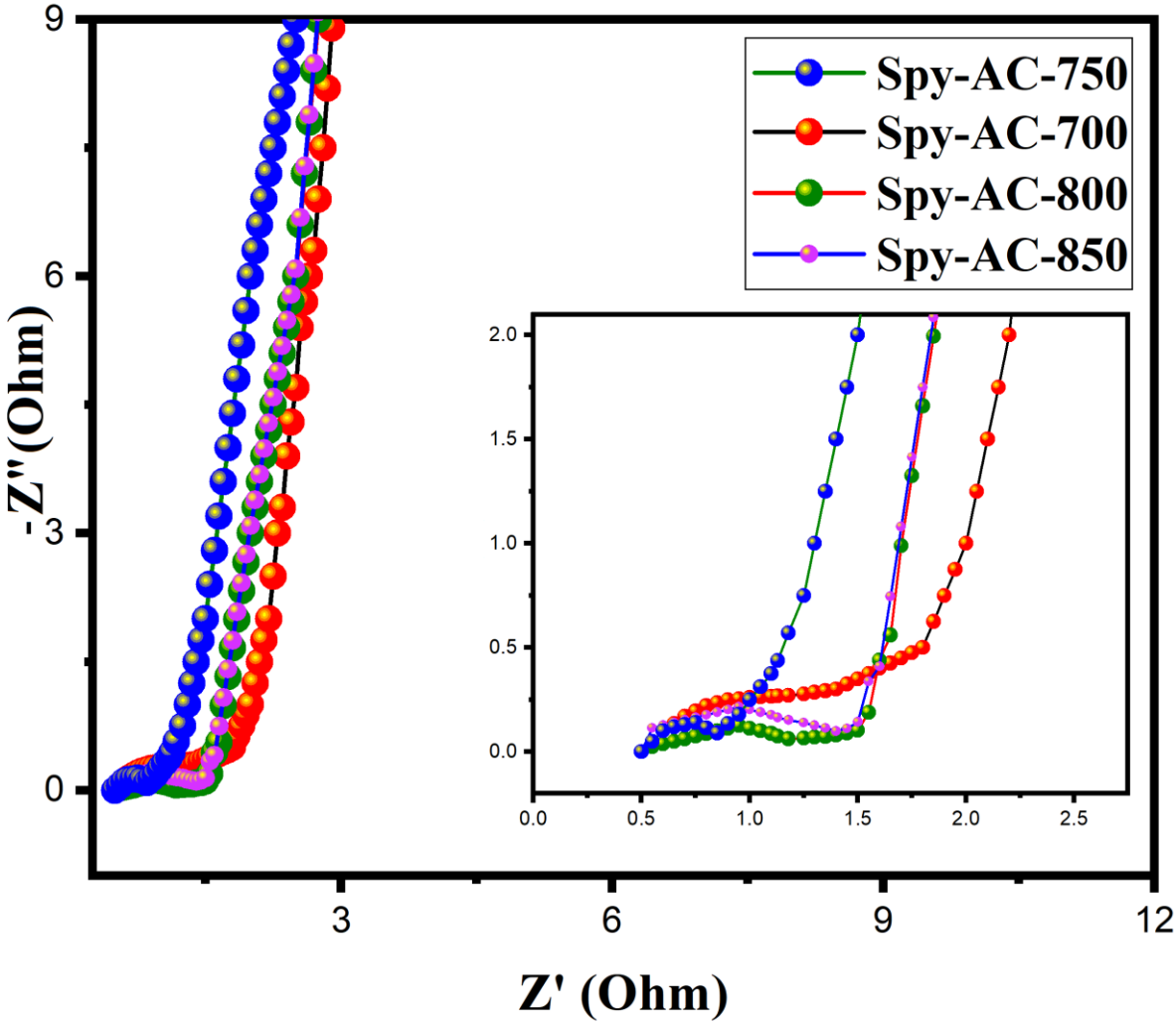

Fig. 4-13: The Nyquist curves for Spy-AC-700, Spy-AC-750, Spy-AC-800 and Spy-AC-850 applied

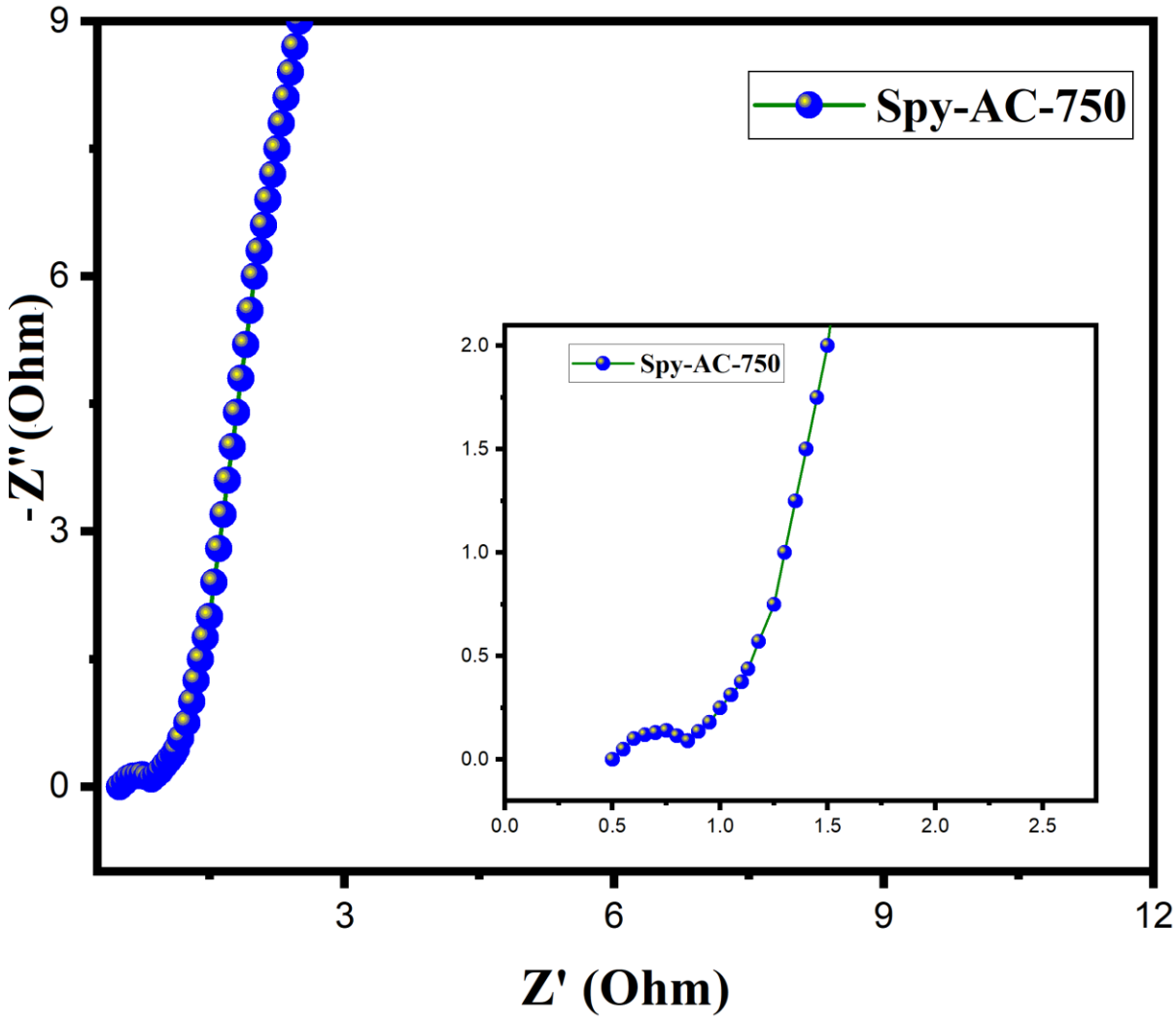

Fig. 4-14: Nyquist plot of Spy-AC-750

To analyze the stability of the Spy AC-750 applied electrode in the three electrode system, a cyclic stability test was performed at a current rate of 1.0 $A.g^{-1}$. Fig. 4.15 shows that the value of specific capacitance gradually decreases with the increase in number of cycles. The curve shows that even after 5000 cycles, the performance of the capacitor remains 79% showing a strong cyclic stability characteristic for a supercapacitor. This stable electrochemical performance occur with prolonged cycling and stable specific capacitance[37].

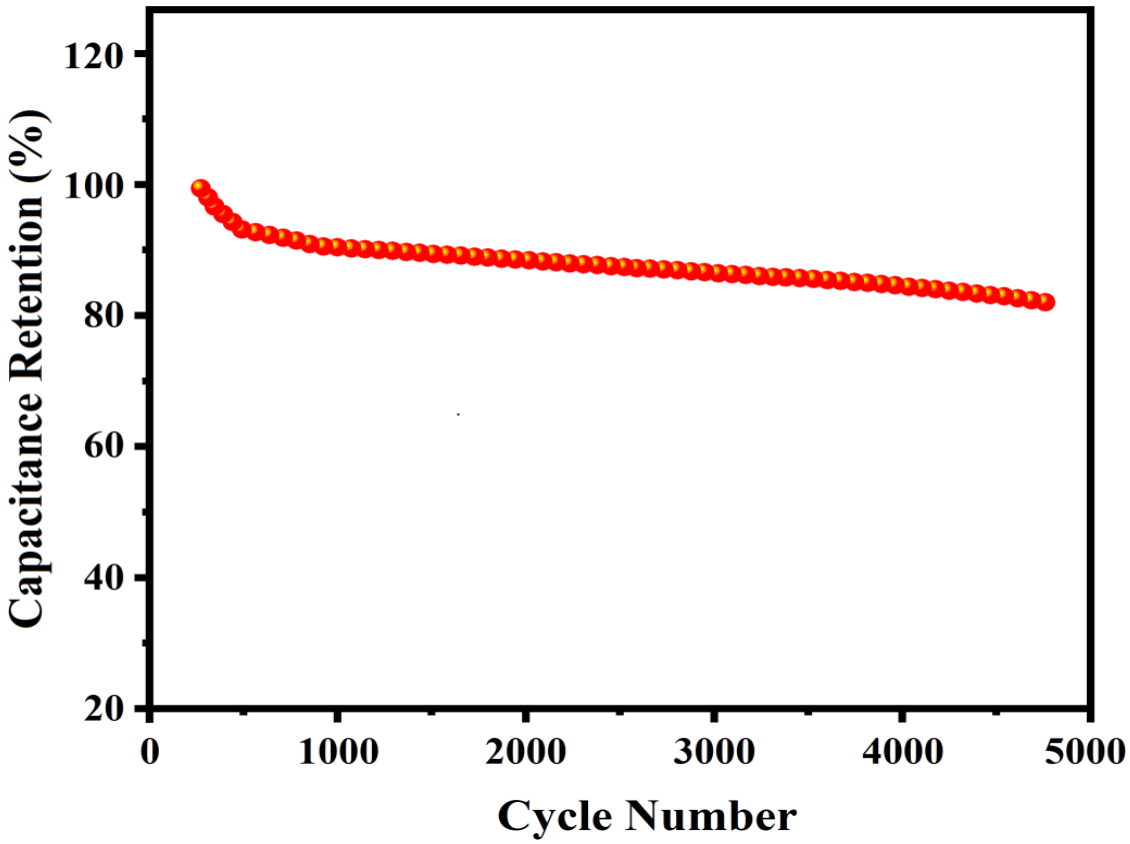

Fig. 4-15: Cyclic stability curve of Spy-AC-750

Summary

This chapter comprises the detailed discussion about various results of *Spirogyra* derived activated carbon. Morphological analysis was conducted to study various structural features of algae, synthesized biochar and activated carbon using SEM. TGA analysis was conducted to study the property of weight loss and thermal stability of algae and Spy-AC-750. The crystal structure characterization of Spy-AC-750 at micro level was reviewed by XRD patterns. Presence of various functional groups in the Spy AC-750 was detected through FTIR spectrum. To investigate the structural features like stability and vibrational response of Spy-AC-750, Raman spectroscopy was applied at 531.82nm laser wavelength. The BET method and pore size distributions are the two basic approaches used to characterize the porous structures of activated carbon. BJH method was used to analyze pore size distribution. The Electrochemical performance of *Spirogyra* Algae derived AC prepared at different temperatures was studied using cyclic voltammetry of AC applied electrodes in three electrode system. The charge capacitance of the material used in the electrodes of storage devices is determined through GCD testing. To identify and assess the electrochemical conductivity and resistance of the electrode, an EIS study was performed. Cyclic stability test was performed to analyze the stability and performance of the supercapacitor even after 5000 cycles.

.

References

[1] W. Jiang, J. Pan, and X. Liu, "A novel rod-like porous carbon with ordered hierarchical pore structure prepared from Al-based metal-organic framework without template as greatly enhanced performance for supercapacitor," 2018, doi: 10.1016/j.jpowsour.2018.10.086.

[2] J. Li, W. Liu, D. Xiao, and X. Wang, "Oxygen-rich hierarchical porous carbon made from pomelo peel fiber as electrode material for supercapacitor," *Appl. Surf. Sci.*, vol. 416, pp. 918–924, 2017, doi: 10.1016/j.apsusc.2017.04.162.

[3] C. Qin *et al.*, "Hierarchical porous carbon derived from Gardenia jasminoides Ellis flowers for high performance supercapacitor," *J. Energy Storage*, vol. 33, no. November 2020, p. 102061, 2021, doi: 10.1016/j.est.2020.102061.

[4] J. Romanos *et al.*, "Nanospace engineering of KOH activated carbon," *Nanotechnology*, vol. 23, no. 1, p. 15401, 2011, doi: 10.1088/0957-4484/23/1/015401.

[5] J. Wang and S. Kaskel, "KOH activation of carbon-based materials for energy storage," *J. Mater. Chem.*, vol. 22, no. 45, pp. 23710–23725, 2012, doi: 10.1039/C2JM34066F.

[6] T. Ouyang *et al.*, "Molten salt synthesis of nitrogen doped porous carbon: a new preparation methodology for high-volumetric capacitance electrode materials," *J. Mater. Chem. A*, vol. 4, no. 25, pp. 9832–9843, 2016, doi: 10.1039/C6TA02673G.

[7] W. Jiang *et al.*, "Hollow-tubular porous carbon derived from cotton with high productivity for enhanced performance supercapacitor," *J. Power Sources*, vol. 438, p. 226936, 2019, doi: https://doi.org/10.1016/j.jpowsour.2019.226936.

[8] T. R. Kumar, R. A. Senthil, Z. Pan, J. Pan, and Y. Sun, "A tubular-like porous carbon derived from waste American poplar fruit as advanced electrode material for high-performance supercapacitor," *J. Energy Storage*, vol. 32, no. September, p. 101903, 2020, doi: 10.1016/j.est.2020.101903.

[9] H. Li *et al.*, "A novel method to prepare a nanotubes@mesoporous carbon composite material based on waste biomass and its electrochemical performance," *J. Mater. Chem. A*, vol. 5, no. 8, pp. 3875–3887, 2017, doi: 10.1039/C6TA10786A.

[10] S. Ahmed, A. Ahmed, and M. Rafat, "Investigation on activated carbon derived from biomass Butnea monosperma and its application as a high performance supercapacitor electrode," *J. Energy Storage*, vol. 26, no. November, p. 100988, 2019, doi: 10.1016/j.est.2019.100988.

[11] J. Ding *et al.*, "Peanut shell hybrid sodium ion capacitor with extreme energy–power rivals lithium ion capacitors," *Energy Environ. Sci.*, vol. 8, no. 3, pp. 941–955, 2015, doi: 10.1039/C4EE02986K.

[12] A. Lazzarini *et al.*, "A comprehensive approach to investigate the structural and surface properties of activated carbons and related Pd-based catalysts," *Catal. Sci. Technol.*, vol. 6, no. 13, pp. 4910–4922, 2016, doi: 10.1039/c6cy00159a.

[13] S.-W. Han, D.-W. Jung, J.-H. Jeong, and E.-S. Oh, "Effect of pyrolysis temperature on carbon obtained from green tea biomass for superior lithium ion battery anodes," *Chem. Eng. J.*, vol. 254, pp. 597–604, 2014, doi:

https://doi.org/10.1016/j.cej.2014.06.021.

[14] J. L. Figueiredo, “Functionalization of porous carbons for catalytic applications,” *J. Mater. Chem. A*, vol. 1, no. 33, pp. 9351–9364, 2013, doi: 10.1039/C3TA10876G.

[15] D. Bose, S. Sridharan, H. Dhawan, P. Vijay, and M. Gopinath, “Biomass derived activated carbon cathode performance for sustainable power generation from Microbial Fuel Cells,” *Fuel*, vol. 236, no. May 2018, pp. 325–337, 2019, doi: 10.1016/j.fuel.2018.09.002.

[16] C. C. Hu, C. C. Wang, F. C. Wu, and R. L. Tseng, “Characterization of pistachio shell-derived carbons activated by a combination of KOH and CO2 for electric double-layer capacitors,” *Electrochim. Acta*, vol. 52, no. 7, pp. 2498–2505, 2007, doi: 10.1016/j.electacta.2006.08.061.

[17] A. G. Pandolfo and A. F. Hollenkamp, “Carbon properties and their role in supercapacitors,” *J. Power Sources*, vol. 157, no. 1, pp. 11–27, 2006, doi: https://doi.org/10.1016/j.jpowsour.2006.02.065.

[18] S. Rawal, B. Joshi, and Y. Kumar, “Synthesis and characterization of activated carbon from the biomass of Saccharum bengalense for electrochemical supercapacitors,” *J. Energy Storage*, vol. 20, no. October, pp. 418–426, 2018, doi: 10.1016/j.est.2018.10.009.

[19] T. Chen *et al.*, “Thalia dealbata Inspired Anisotropic Cellular Biomass Derived Carbonaceous Aerogel,” *ACS Sustain. Chem. Eng.*, vol. 6, no. 12, pp. 17152–17159, Dec. 2018, doi: 10.1021/acssuschemeng.8b04528.

[20] Y. Liu, Z. Shi, Y. Gao, W. An, Z. Cao, and J. Liu, “Biomass-Swelling Assisted Synthesis of Hierarchical Porous Carbon Fibers for Supercapacitor Electrodes,” *ACS Appl. Mater. Interfaces*, vol. 8, no. 42, pp. 28283–28290, Oct. 2016, doi: 10.1021/acsami.5b11558.

[21] E. Lei, W. Li, C. Ma, Z. Xu, and S. Liu, “CO 2 -activated porous self-templated N-doped carbon aerogel derived from banana for high-performance supercapacitors,” *Appl. Surf. Sci.*, vol. 457, no. April, pp. 477–486, 2018, doi: 10.1016/j.apsusc.2018.07.001.

[22] Z. Zou, X. Luo, L. Wang, Y. Zhang, Z. Xu, and C. Jiang, “Highly mesoporous carbons derived from corn silks as high performance electrode materials of supercapacitors and zinc ion capacitors,” *J. Energy Storage*, vol. 44, no. PA, p. 103385, 2021, doi: 10.1016/j.est.2021.103385.

[23] C. Namasivayam and D. Sangeetha, “Recycling of agricultural solid waste, coir pith: Removal of anions, heavy metals, organics and dyes from water by adsorption onto ZnCl2 activated coir pith carbon,” *J. Hazard. Mater.*, vol. 135, no. 1–3, pp. 449–452, 2006, doi: 10.1016/j.jhazmat.2005.11.066.

[24] R. Acosta, V. Fierro, A. Martinez de Yuso, D. Nabarlatz, and A. Celzard, “Tetracycline adsorption onto activated carbons produced by KOH activation of tyre pyrolysis char,” *Chemosphere*, vol. 149, pp. 168–176, 2016, doi: https://doi.org/10.1016/j.chemosphere.2016.01.093.

[25] L. Wan *et al.*, “Multi-heteroatom-doped hierarchical porous carbon derived from chestnut shell with superior performance in supercapacitors,” *J. Alloys Compd.*, vol. 790, pp. 760–771, 2019, doi: https://doi.org/10.1016/j.jallcom.2019.03.241.

[26] B. Liu, Y. Liu, H. Chen, M. Yang, and H. Li, "Oxygen and nitrogen co-doped porous carbon nanosheets derived from Perilla frutescens for high volumetric performance supercapacitors," *J. Power Sources*, vol. 341, pp. 309–317, 2017, doi: https://doi.org/10.1016/j.jpowsour.2016.12.022.

[27] S. Ahmed, M. Parvaz, R. Johari, and M. Rafat, "Studies on activated carbon derived from neem (azadirachta indica) bio-waste, and its application as supercapacitor electrode," *Mater. Res. Express*, vol. 5, no. 4, 2018, doi: 10.1088/2053-1591/aab924.

[28] F. Boudrahem, F. Aissani-Benissad, and H. Aït-Amar, "Batch sorption dynamics and equilibrium for the removal of lead ions from aqueous phase using activated carbon developed from coffee residue activated with zinc chloride," *J. Environ. Manage.*, vol. 90, no. 10, pp. 3031–3039, 2009, doi: https://doi.org/10.1016/j.jenvman.2009.04.005.

[29] J. Du, L. Liu, Y. Yu, Z. Hu, B. Liu, and A. Chen, "N-Doped Hollow Carbon Spheres/Sheets Composite for Electrochemical Capacitor," *ACS Appl. Mater. Interfaces*, vol. 10, no. 46, pp. 40062–40069, Nov. 2018, doi: 10.1021/acsami.8b16921.

[30] Z. Bi *et al.*, "Biomass-derived porous carbon materials with different dimensions for supercapacitor electrodes: a review," *J. Mater. Chem. A*, vol. 7, no. 27, pp. 16028–16045, 2019, doi: 10.1039/C9TA04436A.

[31] S. Osman, Senthil, J. Pan, and Y. Sun, "A novel coral structured porous-like amorphous carbon derived from zinc-based fluorinated metal-organic framework as superior cathode material for high performance supercapacitors," *J. Power Sources*, vol. 414, pp. 401–411, Feb. 2019, doi: 10.1016/j.jpowsour.2019.01.026.

[32] A. Apriwandi, E. Taer, R. Farma, R. N. Setiadi, and E. Amiruddin, "A facile approach of micro-mesopores structure binder-free coin/monolith solid design activated carbon for electrode supercapacitor," *J. Energy Storage*, vol. 40, no. March, p. 102823, 2021, doi: 10.1016/j.est.2021.102823.

[33] P. Manasa, Z. J. Lei, and F. Ran, "Biomass Waste Derived Low Cost Activated Carbon from Carchorus Olitorius (Jute Fiber) as Sustainable and Novel Electrode Material," *J. Energy Storage*, vol. 30, no. April, p. 101494, 2020, doi: 10.1016/j.est.2020.101494.

[34] C. Zequine *et al.*, "High-Performance Flexible Supercapacitors obtained via Recycled Jute: Bio-Waste to Energy Storage Approach," *Sci. Rep.*, vol. 7, no. 1, pp. 1–12, 2017, doi: 10.1038/s41598-017-01319-w.

[35] M. Wu *et al.*, "Pore regulation of wood-derived hierarchical porous carbon for improving electrochemical performance," *J. Energy Storage*, vol. 40, no. April, p. 102663, 2021, doi: 10.1016/j.est.2021.102663.

[36] X. Tian *et al.*, "Flute type micropores activated carbon from cotton stalk for high performance supercapacitors," *J. Power Sources*, vol. 359, pp. 88–96, 2017, doi: 10.1016/j.jpowsour.2017.05.054.

[37] A. Jain, M. Ghosh, M. Krajewski, S. Kurungot, and M. Michalska, "Biomass-derived activated carbon material from native European deciduous trees as an inexpensive and sustainable energy material for supercapacitor application," *J. Energy Storage*, vol. 34, no. September 2020, p. 102178, 2021, doi: 10.1016/j.est.2020.102178.

Chapter 5

Conclusions and Recommendations

5.1. Conclusions

In this study the focus has been on the synthesis of activated carbon derived from abundantly available biomass precursor i.e. fresh water green algae "*Spirogyra*" as well as on the use of activated carbon as an electrode material for supercapacitor application. The process of KOH activation has enhanced the physical/morphological and chemical characteristics such as surface area, porosity, specific capacitance and electrical conductivity. As among the four synthesized samples of activated carbon, Spy-AC-750 has the remarkable surface area (BET) of 727.765 m^2/g having total pore volume of 0.317 (cm^3/g). Spy-Ac-750 has the characteristic of supercapacitive nature having specific capacitance of 210 F/g at 0.5 A/g. Considering the abundance and easy availability, practically economical, environmentally safer, and without any practical investments are the main sorts to consider *Spirogyra* as a precursor for the synthesis of activated carbon. However the TGA plot reveals that only a very small amount of activated carbon (4-5 %) remains after carbonization and activation at 750°C, which is the main discouraging aspect of using *Spirogyra* algae for the synthesis of activated carbon.

5.2. Recommendations

- High surface area activated carbon has a huge potential for its use in various practical applications especially in energy storage devices as electrode material as well as absorbent in the devices used for purification.
- *Spirogyra*, as a cheap and abundantly available biomass precursor, can be easily transformed into high surface area activated carbon making it even more promising for supercapacitor application.
- The morphological and electrochemical results of *Spirogyra* derived activated carbon are acceptable and comparable to the commercially available alternatives.

Appendix 1 – Publications

Optimized synthesis and characterization of *spirogyra* derived activated carbon for high performance supercapacitors

ABSTRACT

This study describes the synthesis of *Spirogyra*-derived activated carbon via two key steps of carbonization and activation at an optimized temperature using KOH as an activation agent, as well as its application in supercapacitors. Surface structure and morphology of activated carbon were examined using SEM, TGA, XRD, FTIR, Raman spectroscopy, and BET surface area, while electrochemical behavior was studied using CV, GCD, and EIS. Specific surface area of Spy-AC-750 calculated was 727.765 m^2g^{-1} with a total pore volume of 0.317 cm^3g^{-1}. The Spy-AC-750 coated electrode attained a specific capacitance of 210 Fg^{-1} at a scan rate of $0.5g^{-1}$. The electrochemical behavior of the Spy-AC-750 coated electrodes was also tested practically by making symmetric device. The excellent results obtained are the key factors to consider Spy-AC-750 as a good electrode material. Conversely the low carbon content is the key discouraging aspect of spirogyra algae to use as a precursor for the synthesis of activated carbon.

Key words:

Spirogyra Algae, Algal biomass derived activated carbon, Supercapacitor, EDLC, KOH as activating agent, Cyclic Voltammetry, BET analysis

Journal: **Waste and Biomass Valorization**

Impact Factor: **3.575**

Status: **Under Review**

`